

## **Abstract**

Telecommunications is a growing and intensely competitive global multi-trillion dollar industry that specializes in the transmission of information all over the world. The data for every television show, website, and telephone conversation travels through one of the industrys many information networks. One of the most common methods of transmission is using fiber optic networks, in which a laser is modulated to send light signals into an optical fiber. The importance of vertical-cavity surface-emitting lasers (VCSELs) to the telecommunications industry is growing rapidly. VCSELs are more cost-efficient to mass-produce and they have better fiber coupling efficiencies as compared to the edge-emitting semiconducting lasers that are the current industry standard.

VCSELs were developed with the hope that they would not be subject to some of the main failings of edge-emitting lasers, such as sensitivity to optical feedback. This occurs when some of the emitted light from a laser is accidentally reflected off other optical components in a system, like the end of an optical fiber, back into the laser. The space between the aperture of the laser and the reflective surface is defined as an external cavity. Extremely-short external-cavity (ESEC) optical feedback is feedback that occurs from a surface within a few microns of the VCSEL aperture.

In an unmodulated VCSEL, ESEC feedback has been shown to produce periodic variation in the VCSEL's threshold current, output power [1], polarization switching current and polarization switching current hysteresis width [2], with respect to variation in the external cavity length. The experimental setup for this experiment mimics the operational setup of a modulated fiber coupled VCSEL as it would be used for data transmission. This presentation will examine those same laser characteristics under the effects of ESEC optical feedback on VCSELs modulated up to 10 GHz.

**THE EFFECTS OF EXTREMELY-SHORT  
EXTERNAL CAVITY OPTICAL  
FEEDBACK INTO A MODULATED  
VERTICAL-CAVITY SURFACE-EMITTING  
LASER**

**Elizabeth Merritt**

Department of Physics

Mount Holyoke College

May 2007

Advisor: Janice Hudgings

Associate Professor of Physics

Mount Holyoke College

A thesis presented to the faculty of Mount Holyoke College in  
partial fulfillment of the requirements for the degree of Bachelor of  
**Arts.**

## 0.1 ACKNOWLEDGEMENTS

I would like to thank my advisor Prof. Janice Hudgings for giving me the amazing opportunity to work with her for the past few years. The experiment may not have always run smoothly, but the experience itself was priceless. Thank you, Janice.

Thank you to Prof. Harriet Pollatsek and Prof. Mark Peterson for serving on my thesis committee.

I would also like to thank my labmates, Evelyn Kapusta, Diane Crenshaw, and especially Katie Greenberg and Adam Kaplan, as well as the very wise Maryam Farzenah. Katie, Adam, and Maryam, thank you for reassuring and putting up with me when the experiment wasn't working.

Thank you to Prof. Shubha Tewari for being so understanding about my non-existent homework for the last couple weeks. Also, thank you for all the help and time you've given me, even when it had nothing to do with what we were learning in class.

Thank you to the entire physics community at MHC. You were the highlight of my years here. I'll always remember the department as a kind of surrogate family. I'll miss the time spent in the lounge together doing the endless homework sets, or just dancing or talking and getting each other through. Finally, thank you to my family, Peter, Aurora and Ariel for supporting me through all the times when I thought I just might not be able to pull this off.

# Contents

0.1	ACKNOWLEDGEMENTS . . . . .	1
	<b>1 INTRODUCTION</b>	<b>9</b>
	<b>2 LASER FUNDAMENTALS</b>	<b>15</b>
2.1	The Fabry-Perot Resonator . . . . .	15
2.2	The Gain Region . . . . .	18
2.2.1	Material Properties . . . . .	19
2.2.2	Carriers in the Gain Region . . . . .	22
2.2.3	Gain/Absorption Mechanisms . . . . .	24
2.2.4	Coherence . . . . .	28
2.2.5	Gain Curves . . . . .	30
2.3	The Lasing Frequency . . . . .	32
2.4	Loss and Lasing . . . . .	33
2.4.1	Summary . . . . .	36
2.5	Laser Rate Equations . . . . .	37

	3
2.5.1 Steady-State Solutions . . . . .	40
2.5.2 Modulation . . . . .	42
2.6 VCSEL Fundamentals . . . . .	45
2.6.1 VCSEL Lasing Frequency . . . . .	46
2.6.2 Bragg Mirrors . . . . .	47
2.7 Polarization . . . . .	53
2.8 Conclusion . . . . .	53
<b>3 FEEDBACK</b>	<b>54</b>
3.1 Derivation . . . . .	56
3.2 Steady-State Solutions with Feedback . . . . .	64
3.3 Summary . . . . .	69
<b>4 Experiment</b>	<b>70</b>
4.1 Experimental setup . . . . .	71
4.2 Experiment . . . . .	75
4.3 Coherence Length . . . . .	77
4.4 Polarization . . . . .	78
4.5 Threshold Current . . . . .	84
4.6 Power . . . . .	85
4.7 Wavelength . . . . .	93
<b>5 CONCLUSION</b>	<b>97</b>

# List of Figures

2.1	Basic Laser . . . . .	16
2.2	Fabry-Perot Resonator . . . . .	16
2.3	Fabry-Perot Frequencies in an Idealized Zero-loss Cavity . . . . .	18
2.4	Broadened Fabry-Perot Frequencies . . . . .	18
2.5	Atom Energy Diagram . . . . .	19
2.6	Crystal Energy Diagram . . . . .	20
2.7	Conductor Energy Diagram . . . . .	21
2.8	Insulator Energy Diagram . . . . .	21
2.9	Semiconductor Energy Diagram . . . . .	22
2.10	Simple Semiconductor Energy Diagram . . . . .	22
2.11	Spontaneous Emission . . . . .	25
2.12	Spontaneous Absorption . . . . .	25
2.13	Stimulated Emission . . . . .	26
2.14	Gain Curve . . . . .	31
2.15	Gain Curves with Changing Current( $I$ ) . . . . .	31

2.16 Lasing Frequency . . . . .	32
2.17 Gain vs. Loss . . . . .	34
2.18 Idealized Gain vs. Current . . . . .	36
2.19 Idealized Optical Output vs. Current . . . . .	36
2.20 Calculated Power vs. Current (LI) Curve . . . . .	42
2.21 Calculated Voltage vs. Current (VI) Curve . . . . .	43
2.22 Sinusoidal Injection Current versus Time for $f = 2\text{GHz}$ . . . . .	44
2.23 Solution for Carrier Density with a Sinusoidal Injection Current for $f = 2\text{GHz}$ . . . . .	44
2.24 Solution for Photon Density with a Sinusoidal Injection Current for $f = 2\text{GHz}$ . . . . .	45
2.25 VCSEL Structure . . . . .	46
2.26 VCSEL Lasing Frequency . . . . .	47
2.27 Reflection from a boundary . . . . .	48
2.28 Bragg Mirror Layers . . . . .	49
2.29 Light Paths for Case 1 . . . . .	50
2.30 Light Paths for Case 2 . . . . .	52
3.1 Feedback from a Fiber to a VCSEL . . . . .	55
3.2 Three Cavity System . . . . .	55
3.3 Laser with Effective Mirror . . . . .	59
3.4 Calculated Carrier Density vs. External Cavity Length . . . . .	65

3.5	Calculated Photon Density vs. External Cavity Length . . . . .	66
3.6	Calculated Gain vs. External Cavity Length . . . . .	67
3.7	Calculated Threshold Current Shift due to Feedback . . . . .	67
4.1	Experimental Setup: The laser control section of the setup controls the temperature and injection current of the VCSEL. The fiber positioning section adjusts the fiber facet until it is aligned normal to the laser beam. The detection and analysis section records measurements of the properties of the output beam, such as power, modulation frequency, lasing wavelength, and polarized power. Table 4.1 is a list of the equipment. . . . .	72
4.2	Comparison of the Spectral Width of the VCSEL for no modulation, 40MHz, and 2.6GHz . . . . .	77
4.3	LI curves for the X and Y polarizations of a VCSEL . . . . .	79
4.4	LI curves for the X and Y polarizations of a VCSEL with modulation . . . . .	79
4.5	LI curves for the Y polarization of a VCSEL with and without feedback . . . . .	80
4.6	Variation of the Threshold Current with changing External Cavity Length . . . . .	82
4.7	Variation of the Threshold Current with Modulation with changing External Cavity Length . . . . .	82

4.8	Comparison of the Amplitudes of the with and without modulation cases of the Threshold Current variation with Feedback	83
4.9	Variation of the Output Power with changing External Cavity Length . . . . .	86
4.10	Variation of the Output Power with Modulation with changing External Cavity Length . . . . .	86
4.11	Comparison of the Amplitudes of the with and without modulation cases of the Output Power variation with Feedback . . .	87
4.12	Comparison of the amplitudes of the Power variation with feedback for a range of injection currents. . . . .	90
4.13	Comparison of the amplitudes of the Power variation with feedback and modulation for a range of injection currents. . . . .	91
4.14	Comparison of the slopes of the LI curves with feedback for 4 different trials . . . . .	92
4.15	Variation of the Lasing Wavelength with changing External Cavity Length . . . . .	94
4.16	Variation of the Output Power with Modulation with changing External Cavity Length . . . . .	94
4.17	Comparison of the Amplitudes of the with and without modulation cases of the Lasing Wavelength variation with Feedback	95

# List of Tables

2.1	Constant values for MATLAB Simulations [4] . . . . .	41
4.1	Equipment List corresponding to Figure 4.1 . . . . .	73

# Chapter 1

## INTRODUCTION

Telecommunications is a growing and intensely competitive global multi-trillion dollar industry specializing in the transmission of information all over the world. The data for every television show, website, and telephone conversation travels through one of the industry's many information networks. Currently, the competitive edge in the market comes from speed, as companies need much faster and more efficient ways to transmit data. One of the most common methods of transmission is using fiber optic networks, in which a laser sends pulses of light into an optical fiber. The data then travels down the optical fiber to a light-sensitive receiver.

The importance of vertical-cavity surface-emitting lasers (VCSELs) to the telecommunications industry is growing rapidly. VCSELs are more cost-efficient to mass-produce, and have better fiber coupling efficiencies than the

edge-emitting semiconducting lasers that are the current industry standard. Also, VCSELs lase in a single longitudinal mode, and thus are not prone to mode hopping, and have a circularly symmetric output beam that can be tightly focused. Currently, VCSELs power most short-distance (under 300 meter) optical links because they operate in the 850nm transmission window. However, there has been recent progress in the development of VCSELs that operate at the 1310 nm or 1550 nm transmission windows required for long-distance communications.

VCSELs were developed with the hope that they would not be subject to some of the main failings of edge-emitting lasers, such as sensitivity to optical feedback. An edge-emitting laser (EEL) is a semiconductor diode laser where all the mirror reflectivity is due to the index of refraction difference at the air/semiconductor boundary and all the light in the laser propagates horizontally in the laser, not through the diode material. Optical feedback occurs when some of the emitted light from a laser is back-reflected off other optical components in a system, such as the end of an optical fiber, or from an optical disk. VCSEL robustness to optical feedback was originally hypothesized because of their high power reflectivity at the mirrors,  $R \approx .998$ , as opposed to the lower reflectivity of EELs,  $R \approx .4$ . The high reflectivity of the mirrors allows less back-reflected light to enter the VCSEL. The high reflectivity of the mirrors also confines photons within the lasing cavity for a longer period

of time, allowing the back-reflected light to be amplified for longer. Thus, the final magnitude of light in the VCSEL due to feedback is on the order of the magnitude of back-reflected light transmitted into an EEL.

For EELs, feedback from a long external cavity, where the length of the external cavity is large relative to the laser but the back-reflected light still bears a phase relationship to the light inside the laser, has been shown to have pronounced effects on their threshold and spectral characteristics [3]. These effects have been divided into 5 regimes. In regime I, the weakest feedback regime, the width of the lasing frequency either increases or decreases depending upon the phase of the back-reflected light. In regime II, modes from the external cavity appear in the emission spectrum. In regime III, the external cavity modes are suppressed and the lasing frequency width narrows. Next, in regime IV, the lasing spectrum broadens and eventually results in coherence collapse [3]. The strong external feedback regime, regime V, results in the appearance of multiple external modes in the lasing spectrum as well as a broadening of the frequency envelope of the external modes. It has also been shown that for EELs the threshold current of the laser decreases with increasing feedback in all regimes.

Similar feedback regimes have been observed in VCSEL with long cavity feedback ([5],[6],[7]), where the external cavity is large but, unlike the case for the EEL, the back-reflected light bears no strong phase relationship to the

light inside the VCSEL.

In addition to the feedback effects that VCSELS share with EELs, the polarization of a VCSELS light is also affected by optical feedback. A VCSEL lases in one of two possible orthogonal modes. When long cavity external feedback is applied, the laser light begins to hop between those two polarization modes [8] while always lasing exclusively in one mode. Under high-speed current modulation, without feedback, the polarization exclusivity of the laser breaks down and results in the coexistence of the two polarization modes [9]. With long cavity feedback and current modulation, the VCSEL dynamics are determined by the the relative strengths of the modulation and feedback. The modulation and feedback effect the power frequency spectrum, the spectrum of frequency fluctuations in the output power of the laser over time. The power frequency spectrum can be dominated by the frequency of the modulation or the frequency of the external modes, or the modulation and external mode frequencies can coexist in the power frequency spectrum. Which form the power frequency spectrum takes depends on the ratio of the modulation strength to the feedback strength. Weak modulation leads to the dominance of feedback effects, while weak feedback leads to the dominance of modulation effects [10].

Extremely-short external-cavity (ESEC) optical feedback is feedback that occurs from a surface within a few tens of microns of the VCSEL aperture, within the coherence length of the VCSEL. In an unmodulated VCSEL, ESEC

feedback produces sinusoidal variation in the VCSEL's resonant wavelength, threshold current, output power [1], and polarization switching current and hysteresis width [2].

This paper will examine the effects of extremely-short external-cavity (ESEC) optical feedback on modulated Vertical-Cavity Surface-Emitting Lasers (VCSELs). The experiment mimics the conditions a VCSEL would operate under as part of a telecommunications network. An optical fiber is positioned a few tens of microns away from the VCSEL and oriented such that it reflects light back into the VCSEL. This scenario occurs accidentally in telecommunications when an optical fiber is coupled to a laser to allow the laser to send signals into the fiber. The current modulation is what creates that light signal. Examining a modulated VCSEL with ESEC optical feedback serves to characterize whether modulation might amplify the feedback effects and make VCSELs unsuitable for telecommunications.

By deliberately exposing VCSELs modulated at a frequency of 1 GHz to 10 GHz, a desirable range for communication speeds, to different intensities of ESEC optical feedback, we study changes in the properties of the laser such as shifts in threshold current, shifts in the lasing spectrum, changes in the coherence length, and the polarization of the beam so that we can compare these effects to those of an unmodulated VCSEL without feedback.

This paper will show that the effects of optical feedback are less severe

with higher speed modulation because the coherence length of the beam decreases at higher modulation frequencies. With a decrease in the coherence of back-reflected photons, there is reduced interference with the photons in the lasing cavity, reducing the severity of the feedback effects. Thus, modulation of a VCSEL exposed to ESEC optical feedback does not create any additional complications that might reduce the suitability of VCSELs for telecommunications.

## Chapter 2

# LASER FUNDAMENTALS

A basic laser design consists of two mirrors, each of power reflectivity  $R$  surrounding a gain region, as seen in Figure 2.1. The mirrors trap light between them such that the photons constantly travel back and forth between them through the gain region. Under the right conditions, the light is amplified for every pass it makes through the gain region.

### 2.1 The Fabry-Perot Resonator

The two mirrors of the laser trap photons between them and create a classic Fabry-Perot cavity. Assuming all light in the cavity is effectively trapped between the two mirrors, with reflectivity  $R = 100\%$ , then the light propagates on an axis between the two mirrors. The wavelengths of light that survive in the cavity are the standing waves with nodes at the mirrors.

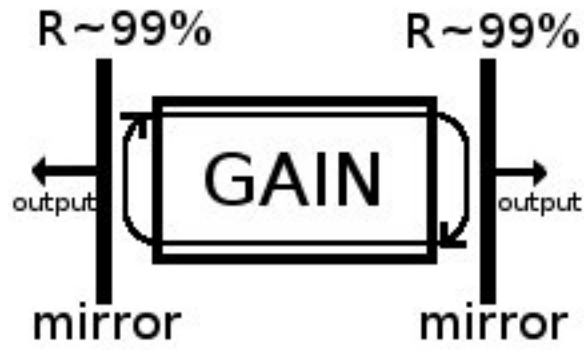


Figure 2.1: Basic Laser

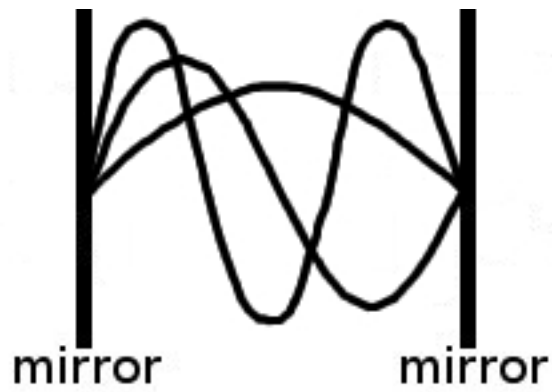


Figure 2.2: Fabry-Perot Resonator

If the mirrors are perfectly reflecting, the standing waves have nodes at the mirrors. Then the standing waves in the cavity have wavelengths

$$\lambda_1 = 2L, \lambda_2 = L, \lambda_3 = \frac{2L}{3}, \dots, \lambda_m = \frac{2L}{m}. \quad (2.1)$$

Since

$$c_n = \lambda f, \quad (2.2)$$

where  $\lambda$  is the wavelength of the light, then

$$f_m = \frac{mc_n}{2L}, \quad (2.3)$$

$$m = 1, 2, 3 \dots \quad (2.4)$$

Therefore, the Fabry-Perot cavity sets up an infinite number of standing waves of evenly spaced frequencies (Figure 2.3), where the distance between frequencies is  $\Delta f = \frac{c_n}{2L}$ . These frequencies are referred to as the longitudinal modes of the laser.

Thus the mirrors of the lasing cavity, with a cavity of length  $L$ , limits the waves inside the cavity to frequencies of  $f_m = \frac{mc_n}{2L}$ , where  $m$  is an integer and  $c_n = \frac{c}{n}$  is the speed of light in a medium with index of refraction  $n$ .

However, it is impossible to build an ideal mirror. Thus the reflectivity of any mirror is  $R < 100\%$ . In this case some light escapes the laser cavity; this is the laser beam. If this were not the case, all the light would just remain trapped in the laser where it could not be used. This non-ideal reflectivity introduces

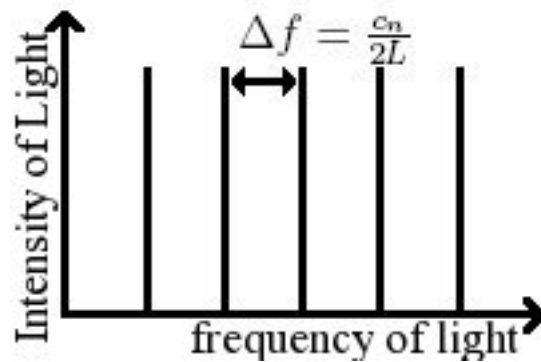


Figure 2.3: Fabry-Perot Frequencies in an Idealized Zero-loss Cavity

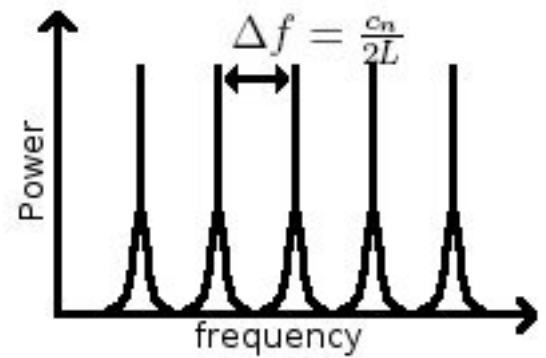


Figure 2.4: Broadened Fabry-Perot Frequencies

some loss into the system and creates some broadening of the frequency lines.

Therefore, the frequency spectrum of a real laser looks more like Figure 2.4 than Figure 2.3.

## 2.2 The Gain Region

As already discussed, the gain region is the region of the laser where photons can be replicated. The gain region only replicates one small spectrum of wavelengths, as determined by the material composition of the region. Gain is defined as the net amplification of light in a laser, the total amplified light minus the total absorbed light.

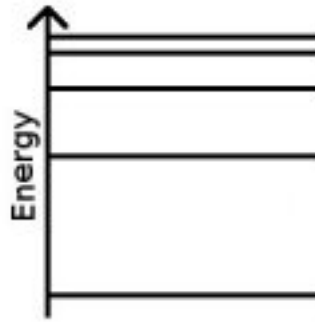


Figure 2.5: Atom Energy Diagram

### 2.2.1 Material Properties

To understand the light replication properties of the gain region in a semiconductor laser, one must first understand the energy states of the gain material. Consider a typical energy diagram of an atom as in Figure 2.5. Each of the horizontal lines represents one of the atom's discrete allowed energy states. Electrons orbiting the atom can only occupy these specific energy levels.

In a crystal, discrete energy states still exist, but the states are packed closely such that a set of the packed states can be taken as a continuous energy band, as seen in Figure 2.6. These close states occur because of the proximity and periodic spacing of atoms in a crystal lattice. The small distance between the atoms allows an electron in one atom to interact with an electron in a neighboring atom.

In a material, electrons fill up the lowest available energy states first

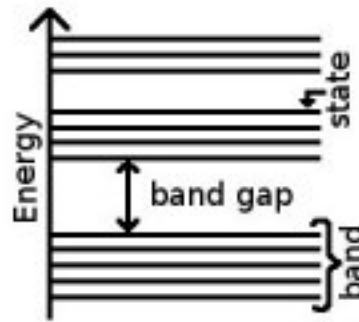


Figure 2.6: Crystal Energy Diagram

in an energy band, with two electrons to a state as dictated by the Pauli Exclusion Principle. The valence band is defined as the highest energy band, at  $T = 0K$ , containing electrons. The conduction band is defined as the first energy band with energy greater than the valence band. The energy difference between the two bands is called the band gap energy,  $E_g$ .

In a conductor, at temperature  $T = 0K$ , the valence band is not completely filled, as seen in Figure 2.7.

Thus, if  $T > 0K$ , then the thermal energy gives electrons in the lower band states enough energy to move into higher empty energy states in the band. By convention, we call empty electron states holes. The electrons in the higher energy states are free to move around in the material. Generally, electrons are always mobile in a conductor.

In an insulator, at  $T = 0K$ , the valence band is completely filled, as seen in Figure 2.8. An insulator also has a large band gap energy. In order for

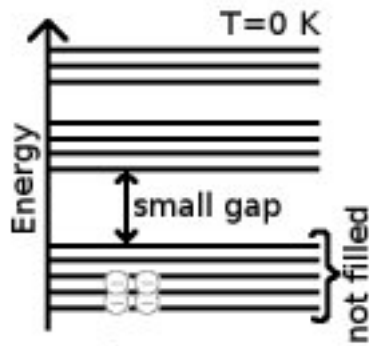


Figure 2.7: Conductor Energy Diagram

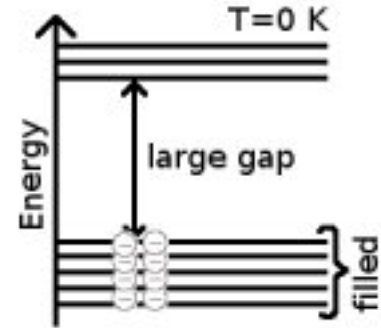


Figure 2.8: Insulator Energy Diagram

electrons to move around, the thermal energy imparted to the electrons must be greater than or equal to  $E_g$ . Since  $E_g$  is large, the energy needed to make electrons flow in the material is large. Generally, electrons cannot flow in an insulator.

A semiconductor has a filled valence band at  $T = 0K$ , but it has a small band gap energy, on the order of  $E_g \approx 1eV$ , as seen in Figure 2.9.

Therefore, it takes a smaller quantity of energy to allow electron movement in the material. A semiconductor does not allow flow of electrons without an applied energy, but the energy needed to allow electron flow is just the small band gap energy.

In practice, energy diagrams of crystalline materials are simplified to only show the allowed energy bands, instead of the individual energy states. Figure 2.10 shows a the simplified, conventional energy diagram for a semi-

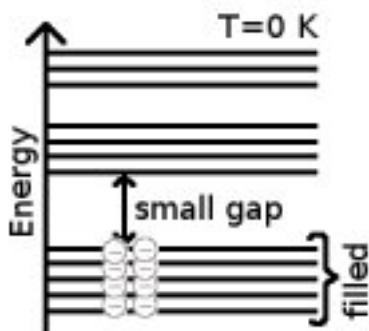


Figure 2.9: Semiconductor Energy Diagram

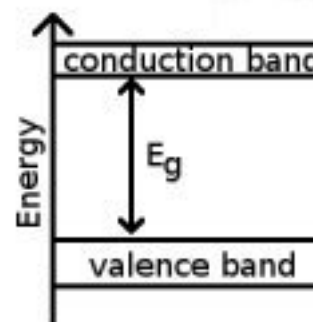


Figure 2.10: Simple Semiconductor Energy Diagram

conductor.

### 2.2.2 Carriers in the Gain Region

The semiconductor lasers discussed in this paper are diode lasers. They consist of a layer of p-doped material, a layer of intrinsic (gain) material, and a layer of n-doped material. A p-doped material is a material in which impurities have been introduced that result in mobile positive charges for the substance. An n-doped material is a material in which the introduced impurities result in mobile negative charges. The negative charges are still referred to as electrons, while the positive charges are referred to as holes. The positive charges are referred to as holes because they represent places an electron could fill. A diode consists of an n-doped material joined to a p-doped material. Sometimes an intrinsic material is inserted between the n-doped and p-doped layers. The intrinsic

material can serve several purposes, such as being structurally favorable for bonding with both the n- and p-doped material when they are not optimal for bonding to each other or to modify the dimensions of a device without significantly changing its electrical properties. In the case of a diode laser, the intrinsic layer consists of the gain material.

A diode has a voltage difference at the p-n junction, or across the intrinsic layer between the p and n materials. The voltage difference represents a build up of electrons and holes at the p-n junction, where the charges have diffused over the junction barrier to the adjoining material and the voltage difference is proportional to the number of charges that diffused out of their original material. In a diode laser this creates a high concentration of electrons and holes in the gain region of the laser. The recombination or creation of electron-hole pairs are responsible for the main gain and absorption mechanisms in the laser. Recombination occurs when an electron fills a hole and the electron-hole pair effectively ceases to exist. Creation occurs when a filled state loses its electron and results in a new electron-hole pair.

A current injected into the diode injects electrons into the n-doped material and pulls electrons out of, or injects holes into, the p-doped material. The combination of the injected electrons from the current and the holes that diffused across the boundary in the n-doped material results in a decrease in the positive charge on that side of the p-n junction. Similarly, the injected

holes and the initially diffused electrons in the p-doped material result in an equal decrease in the charge on the p-side of the p-n junction. The overall decrease in the charge on both sides of the p-n junction decreases any repulsive forces due to the charge buildup. Thus, more electrons and holes can diffuse across the boundary until the repulsive force from the charge buildup is large enough to stop the diffusion of charges across the junction. This creates more electron-hole pairs in the gain region of the laser.

For a VCSEL, the top set of mirrors are fabricated with p-doped materials and the bottom set of mirrors are fabricated with n-doped materials to form the p-n junction required for a diode laser.

### 2.2.3 Gain/Absorption Mechanisms

Three main processes change the amount of light in the laser: spontaneous emission, stimulated emission, and stimulated absorption.

Spontaneous emission requires an electron in the conduction band of the gain material and a hole in the valence band. The electron is in an excited state and, over time, will naturally decay to a lower energy state and recombine with the hole in the valence band. Experimentally, this time is very short, on the order of  $ns$ . The electron decays from the conduction band and recombines with the hole in the valence band, releasing a photon with energy  $E_g$  and a random phase,  $\phi$ , in the process, as seen in Figure 2.11.

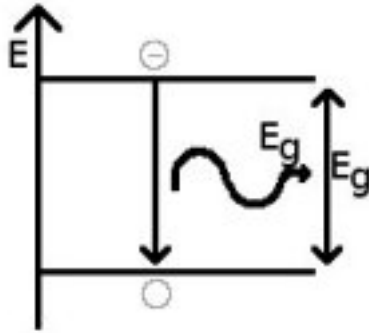


Figure 2.11: Spontaneous Emission

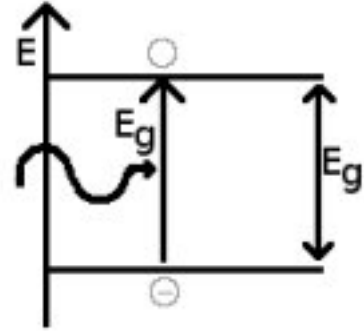


Figure 2.12: Spontaneous Absorption

This process generates light, but the light is only a small source of gain in the laser because of the random direction and phase of the emitted light. The random phase and direction do not ensure that the generated light will remain in the laser as a standing wave, that it will couple into an allowed Fabry-Perot mode. If the photon is not normally incident to the mirrors of the lasing cavity, then it may escape out the sides of the laser. If the phase of the photon does not result in a node at the mirrors, then the photon will not become a standing wave upon reflection. Some fraction of the spontaneously emitted photons do contribute to a lasing mode. This fraction of the photons make spontaneous emission the catalyst for beginning the replication of light.

Stimulated absorption requires an electron in the valence band and a hole in the conduction band. An incident photon with energy  $E_g$  is absorbed by the electron and the electron excites to the conduction band and recombines

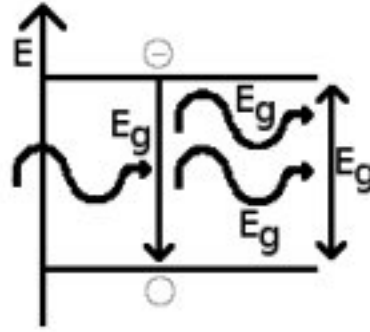


Figure 2.13: Stimulated Emission

with the hole, as seen in Figure 2.12. This mechanism is a small source of light loss in the laser.

Stimulated emission also requires an electron in the conduction band and a hole in the valence band. Unlike spontaneous emission the electron-hole recombination does not occur without some external influence. Instead, a photon with energy  $E_g$  and phase  $\phi$  passes through the material and resonates with the electron in the conduction band. This causes the electron to drop to the valence band. When the electron drops, it emits a photon identical to the incident photon, with energy  $E_g$  and phase  $\phi$ , as seen in Figure 2.13.

When a current is injected into the laser it generates electron-hole pairs in the gain region of the laser that contribute to light absorption and emission. The greater the current, the larger the number of electron hole pairs generated. If the current is increased then the number of electrons in the conduction band increases and the amount of spontaneous emission increases

proportionally. When a larger number of the electrons sit in the conduction band of the material than the valence band, then light emission will be the dominant process in the material. This distribution of electrons-hole pairs is known as population inversion.

If there are electrons in the conduction band, then recombination will spontaneously occur and emit light. Eventually a photon is emitted with a phase and direction such that it couples into one of the allowed lasing modes. If there is population inversion of the electron-hole pairs, then it is probable that the spontaneously emitted light will be amplified by stimulated emission. If there is not population inversion then there is a high probability that the photon will be reabsorbed. If the spontaneously emitted photon is coupled into one of the allowed modes, then all the light from stimulated emission is also coupled into that mode.

Amplification by stimulated emission occurs because most photons created by stimulated emission also induce stimulated emission from other electron-hole pairs as they pass. Thus for any initial photon, stimulated emission replicates it and results in two photons. Each of those two photons are replicated by stimulated emission and result in four photons. This continues to increase geometrically and is only limited by the availability of electrons on the conduction band.

When the light reaches a mirror, it is reflected back through the gain

region. The pass of the light through the gain region continues to increase the amount of light in that mode. The more passes the light makes through the gain region, the more light is generated. This is the primary source of light generation in the laser. Some light is lost at the mirrors for every instance light is reflected, resulting in a relationship between the net generated light and the net light loss. This will be discussed further, later in the chapter.

### 2.2.4 Coherence

Stimulated emission is the primary source of light gain in the laser. This gives laser light unique qualities: monochromaticity, directionality and coherence.

All light created by stimulated emission has the same energy as the original photon. Since  $E = \frac{\hbar c_n}{\lambda}$ , where  $\hbar$  is Planck's constant and  $c_n = c/n$  is the speed of light in a material with index of refraction  $n$ , then all the light has the same wavelength. Since the "color" of light is dependent upon the wavelength of light, all the light generated by stimulated emission is the same color. The light in a lasing mode is created by stimulated emission, thus the light from a laser is monochromatic. Similarly, all laser light possesses the same phase. Unfortunately, no laser is perfectly monochromatic, as will be explained in Section 2.2.5. However, the width of the wavelength spectrum of a laser is small,  $\approx .2nm$ , making a laser effectively monochromatic.

All light trapped in the lasing cavity after several round-trips through

the cavity propagates along the axis normal to the surfaces of the mirrors. Any light that was not on this axis would eventually be reflected out the sides of the laser or not form standing waves and die out due to interference. That light would not contribute to a lasing mode. Thus, all laser light has the same direction, along the axis normal to the laser mirrors.

Any light that has the same wavelength, phase, and direction is known as coherent. Therefore laser light is coherent. Laser light is both spatially and temporally coherent. Spatial coherence means the light at all points in a cross-section of the laser beam is coherent with light at all other points in the cross-section of the beam. Temporal coherence describes the phase correlation between light in one location but at different times. The temporal coherence is normally measured by sending the light through a Michelson interferometer and measuring the visibility of the interference fringes.

The coherence length of the laser is given by  $l_c = c\tau_c$ , where  $l_c$  is the coherence length and  $\tau_c$  is the coherence time.

Unfortunately, laser light is not perfectly coherent. As previously stated, any lasing mode has some finite width, and therefore laser light cannot be perfectly monochromatic. Also, as soon as light exits the laser, it begins to lose coherence due to effects like diffraction from the aperture, and scattering off the air. For a laser these effects are present but relatively small.

### 2.2.5 Gain Curves

One factor overlooked until now is the width of the energy bands. In the previous section it was assumed that all photons had an energy  $E_g$ . Consider an electron that is in the conduction band but is not in the lowest energy state in the band. If the electron decays to the valence band, then the released photon will have some energy  $E_g + \epsilon_1$ , where  $\epsilon_1$  is the energy difference between the lowest energy state in the conduction band and the initial energy state of the electron. Now, consider an electron that is in the lowest state of the conduction band but decays to an energy state in the center of the valence band. The emitted photon must have an energy  $E_g + \epsilon_2$ , where  $\epsilon_2$  is the difference between the highest energy state in the valence band and the final energy state of the electron. Hence, there is a range of energies for both emitted photons. The lower bound of this range is  $E_g$  because the smallest energy of an emitted photon is the energy difference between energy bands. If the energy difference is less than  $E_g$ , then the electron would have to decay to a state within the band gap, but no energy states occur in the band gap.

Statistically, the majority of emitted photons will have an energy slightly larger than  $E_g$  because they can be emitted by electrons in the middle of the conduction band decaying to the middle of the valence band. The probability that the highest states of the conduction band will be occupied or lowest states of the valence band will be empty is small and almost negligible. This results in

a relationship between the number of emitted photons and the photon energy. If each spontaneously emitted photon is replicated by stimulated emission, then the gain, the net increase in emitted photons, is proportional to the number of photons emitted by spontaneous emission. Thus, the gain possess the same general relationship to the photon energy as the number of emitted photons. Figure 2.14 shows the gain versus photon energy curve, which we will refer to as the gain curve.

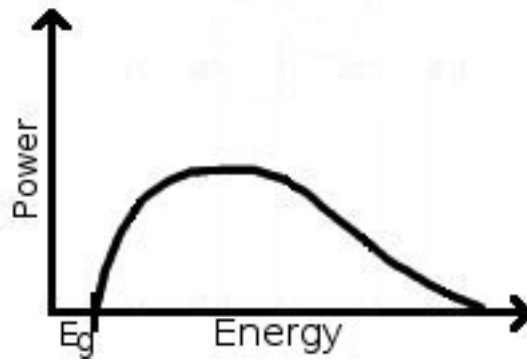


Figure 2.14: Gain Curve

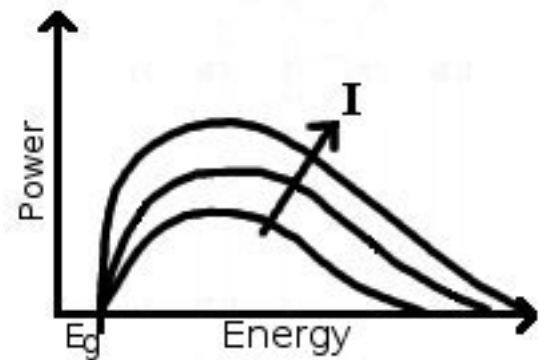


Figure 2.15: Gain Curves with Changing Current ( $I$ )

Gain depends primarily on stimulated emission, and stimulated emission depends on the population of electrons in the conduction band and holes in the valence band. It follows that a change in the population of electrons will produce a change in the gain curve. Initially, it seems that if the current injected into the conduction band increases then the gain should increase uniformly. This is almost correct, but it does not account for the width of the conduction

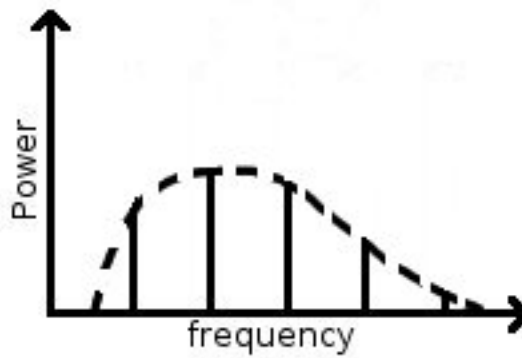


Figure 2.16: Lasing Frequency

band. The current injects electrons into the lowest available energy states. Once an energy state is filled, no more electrons can be injected into it. As the current increases higher energy states fill. Once higher energy states can contribute to emission, then the number of pairs of states with larger energy transitions increases. Higher energy transitions also have a higher number of pairs of initial and final energy states with the corresponding difference in energy. This results in higher energy photons becoming more probable than lower energy photons and skews the gain curve toward higher energies. In general, the gain curve looks like Figure 2.15.

## 2.3 The Lasing Frequency

Section 2.1 established the allowed frequencies of laser light due to the Fabry-Perot cavity created by the mirrors of the laser. Section 2.2.3 established

another set of allowed frequencies constrained by the gain curve of the gain material. Figure 2.16 shows an overlay of these two constraints, Figures 2.3 and 2.14, where the horizontal axis of Figure 2.14 has been converted to frequency.

The only Fabry-Perot modes that could contribute to lasing are the modes with associated frequencies that might be amplified by stimulated emission, the frequencies that fall within the gain spectrum. Any Fabry-Perot modes that fall outside of the gain spectrum can exist, but will not contribute to lasing due to lack of amplification. For some types of lasers such as semiconductor edge-emitting lasers, hundreds of Fabry-Perot modes fall inside the gain spectrum. For edge-emitting lasers,  $\Delta f$  is small due to their relatively large length.

## 2.4 Loss and Lasing

Loss is the percentage of light lost from the Fabry-Perot resonator. The primary source of loss in system is out the mirrors at the end of the cavity due to the imperfect nature of the mirrors. Other sources of loss are stimulated absorption, absorption as heat by the laser and mirror material, imperfect reflection and scattering at the mirrors, and scattering in the laser material. Therefore, there are two different primary processes, gain and loss, that must be taken into account when considering the net light emitted from the laser.

If the gain of one pass of light through the laser cavity is less than the

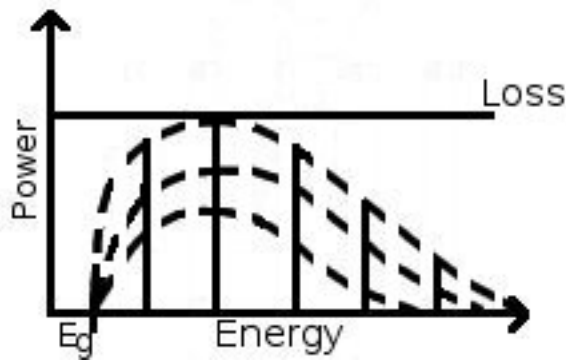


Figure 2.17: Gain vs. Loss

loss, then more light is lost during the trip than is generated by the pass through the gain region. There is a net loss of circulating light in the laser. As long as the system has a net loss of light, no significant amplification due to stimulated emission can occur and the light levels in the laser are small, almost negligible. Thus, the laser cannot lase.

When the current is increased until the gain of at least one lasing mode is equal to the loss of that mode, the laser begins to lase (Figure 2.17). This current is called the threshold current, the current at which the laser "turns on". When gain is equal to loss, then for some initial amount of light in the laser, the number of photons generated due to stimulated emission is equal to the number of photons lost over the course of one full trip through the cavity. This includes the loss out the mirror. The net amount of light left in the laser is then the same as the initial amount; this light is referred to as the circulating power. Therefore, if gain equals loss, then the circulating power is constant.

Similarly, with every pass of light through the laser cavity, the amount of light is emitted through the mirror is constant. This is the laser beam.

It has been experimentally proven that if the injection current, for currents above the threshold current, is increased then the optical output power of the laser increases. Thus, the circulating power within the laser must have increased. This implies that there must have been a momentary net gain in the laser. For the time a net gain in the laser exists, each pass of light through the gain region is slightly larger than the one before. Thus with each pass more electrons are depleted from the conduction band by stimulated emission. Quickly, the amount of circulating light in the cavity is enough that electrons are pulled out of the conduction band as fast as they are pumped in. This point is called gain saturation. Now the loss begins to deplete the number of circulating photons while the conduction band population recovers. The system then settles back to equilibrium where the gain equals the loss but with a larger amount of circulating power.

These fluctuations happen quickly enough that we can consider the gain after threshold to be independent of current. Figure 2.18 shows the complete idealized relationship between gain and input current.

Therefore, the quantity that increases with current is the amount of circulating light. Since the light loss of the mirrors remains constant, the output power increases with increasing current. This relationship is shown in

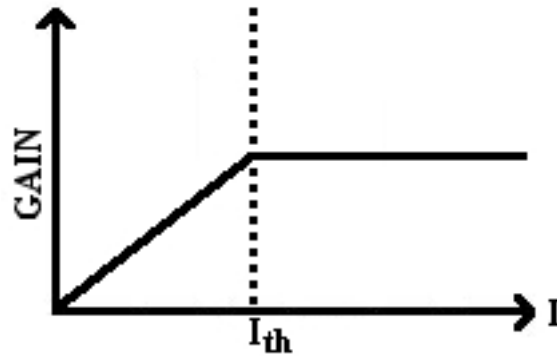


Figure 2.18: Idealized Gain vs. Current

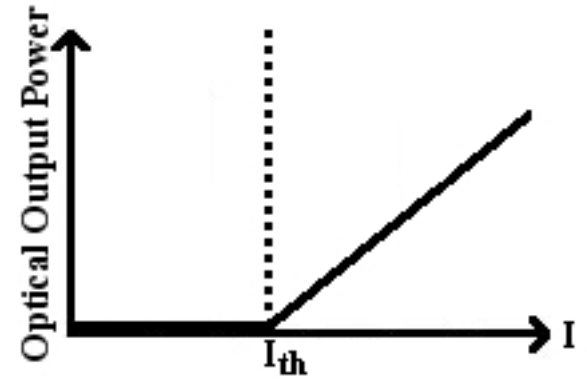


Figure 2.19: Idealized Optical Output vs. Current

Figure 2.19. Figure 2.19 is what is referred to as an LI, for light versus current, curve.

### 2.4.1 Summary

In summary, the Fabry-Perot cavity created by the mirrors restricts the possible lasing frequencies of the laser with respect to those of the standing waves in the cavity. The material composition of the laser further restricts the lasing frequencies by restricting what frequencies will experience gain through stimulated emission. This gain increases with increasing input current as long as the gain of the system is less than its loss. When the gain is equal to the loss, the laser begins to lase and the gain becomes constant. After the laser begins to lase, output power increases linearly with input current.

## 2.5 Laser Rate Equations

The rate equations [4] that describe the interaction of carrier and photons in an operating lasers are

$$\frac{dN}{dt} = \frac{I}{eV} - \frac{N}{\tau} - v_g \frac{dg}{dN} (N - N_{tr})P \quad (2.5)$$

$$\frac{dP}{dt} = v_g \frac{dg}{dN} (N - N_{tr})P\Gamma - \frac{P}{\tau_p} + \beta \frac{N}{\tau} \quad (2.6)$$

where the definitions of each of the terms will be explained below.

The carrier density,  $N$ , is defined as the number of charge carriers per unit volume in the conduction band of the gain region material. The carrier density increases as electrons are injected into the conduction band. This is accounted for by the  $\frac{I}{eV}$  term, where  $I$  is the current, which yields the number of injected charge carriers in the conduction band due to the injection current.

The second term of the carrier density rate equation accounts for the decrease in carrier density from carriers that naturally (spontaneously) decay to the valence band.  $\tau$  is the average amount of time a carrier spends in the conduction band before spontaneously decaying to the valence band. Multiplying the carrier density by  $\frac{1}{\tau}$  gives the rate at which carrier are lost from the conduction band to due to spontaneous emission.

The third term of the carrier density rate equation accounts for the decrease in carrier density due to stimulated emission. Thus, the term is proportional to the photon density,  $P$ , the number of photons per unit volume

in the lasing cavity. Every photon that is created by stimulated emission corresponds to the loss of an electron from the conduction band. Thus, the decrease in the carrier density due to stimulated emission is the negative of increase in photon density due to stimulated emission. The gain function gives the percent increase in the amount of photons as they pass through the gain region. This gain as a function of carrier density can be approximated as a straight line of the form

$$g \approx \frac{dg}{dN}(N - N_{tr}) \quad (2.7)$$

where the differential gain is the slope of the line and the transparency carrier density is defined as the carrier density at which the rate of stimulated absorption equals the rate of stimulated emission and therefore the gain is zero. The term  $\frac{dg}{dN}(N - N_{tr})P$  describes the number of photons generated per unit distance as the photons travel through the gain region. Then, the rate at which photons are generated with respect to time is the gain multiplied by the distance the photons travel per unit time. The average of all photon velocities in the lasing cavity is the photon group velocity. Thus, the final rate of carrier decay due to stimulated emission is  $-v_g \frac{dg}{dN}(N - N_{tr})P$ .

Similarly, the first term of the photon density rate equation is the contribution from the stimulated emission. In this case, the term is multiplied by  $\Gamma$ , the confinement factor. The confinement factor is defined as the ratio of the gain region volume,  $V$ , the volume in which photons are generated, to

the total volume,  $V_p$ , that photons may occupy in the laser:  $\Gamma = \frac{V}{V_p}$ . While the carriers are confined to a narrow gain region, the photons fill the whole laser cavity. The confinement factor corrects for the stimulated emission only taking place in the gain region, not the entire lasing cavity.

The second term of the photon density rate equation is analogous to the second term of the carrier density rate equation. The photon lifetime  $\tau_p$  is the average amount of time a photon spends in the lasing cavity before it is lost to absorption or leaves the laser. Then, multiplying  $P$  by this factor yields the rate at which the photon density is diminished due to absorption or emission.

The third term of the photon density rate equation comes from spontaneous emission within the laser. The spontaneous emission factor,  $\beta$  is defined as the fraction of spontaneously emitted photons that contribute to the lasing mode. As previously stated,  $\frac{N}{\tau}$  is the rate at which carriers decay and produce photons by spontaneous emission. Thus, this term gives the rate at which the fraction of spontaneously emitted photons that contribute to lasing are generated.

These rate equations can be used to predict the behavior of the laser with respect to injection current, such as the relationships of power and voltage to current. For a DC signal, the rate equations predict the characteristic power versus current and power versus voltage behaviors of a laser.

### 2.5.1 Steady-State Solutions

The rate equations for the steady-state are

$$0 = \frac{I}{eV} - \frac{N}{\tau} - v_g \frac{dg}{dN} (N - N_{tr}) P \quad (2.8)$$

$$0 = v_g \frac{dg}{dN} (N - N_{tr}) P \Gamma - \frac{P}{\tau_p} + \beta \frac{N}{\tau}. \quad (2.9)$$

Solving these equations for  $P(N, I)$  we find

$$P(I, N) = \frac{\frac{I}{eV} - \frac{N}{\tau}}{v_g \frac{dg}{dN} (N - N_{tr})} \quad (2.10)$$

Similarly, the solution for  $N(P, I)$  is

$$N(I, P) = \frac{\tau}{\beta} \left[ \frac{P}{\tau_p} - v_g \frac{dg}{dN} (N - N_{tr}) P \right] \quad (2.11)$$

$$= \frac{\tau}{\beta} \left[ \frac{P}{\tau_p} - v_g \frac{dg}{dN} (N - N_{tr}) \frac{\frac{I}{eV} - \frac{N}{\tau}}{v_g \frac{dg}{dN} (N - N_{tr})} \right] \quad (2.12)$$

$$= \frac{\tau}{\beta} \left[ \frac{P}{\tau_p} - \Gamma \left( \frac{I}{eV} - \frac{N}{\tau} \right) \right] \quad (2.13)$$

$$N \left( 1 - \frac{\Gamma}{\beta} \right) = \frac{\tau}{\beta} \left[ \frac{P}{\tau_p} - \Gamma \frac{I}{eV} \right] \quad (2.14)$$

$$N = \frac{\tau}{\beta - \Gamma} \left[ \frac{P}{\tau_p} - \Gamma \frac{I}{eV} \right] \quad (2.15)$$

Numerical analysis of these equations using a MATLAB program, with the physical constants listed in Table 2.1, was able to reproduce the typical light (power) versus current curve characteristic of a laser, as well as the typical voltage versus current curve. Figure 2.20 shows the calculated curve of photon density versus injection current. The light output of the laser is proportional to the photon density in the laser. Thus, Figure 2.20 depicts the general relationship of the output power of the laser to the injection current. Similarly,

$N_{tr}$	$1.8 \times 10^{18}$ carriers per $cm^3$
$v_g$	$3 \times 10^{10}$ cm/s
$\Gamma$	.0382
$\tau$	2.63 ns
$\tau_p$	2.20 ps
$\beta$	$1.69 \times 10^{-4}$
$\frac{dg}{dN}$	$5.10 \times 10^{-16} cm^2$
$\lambda$	850nm

Table 2.1: Constant values for MATLAB Simulations [4]

Figure 2.21 is a graph of the calculated carrier density versus injection current, where voltage is proportional to carrier density.

The linear nature of the LI curve allows identification of the threshold current, in Figure 2.20 the point at which the slope of the curve became noticeably greater than zero. On a calculated LI curve, the threshold current is easily identified. On an experimentally obtained LI curve, spontaneous emission increases the curvature of the curve near threshold, making the threshold current harder to identify. Fortunately, a linear fit of the curve above threshold can be used to calculate the threshold current of an experimental LI curve.

Modifications of these equations, and the corresponding program, will be used to show the effects of modulation and feedback on the behavior of the

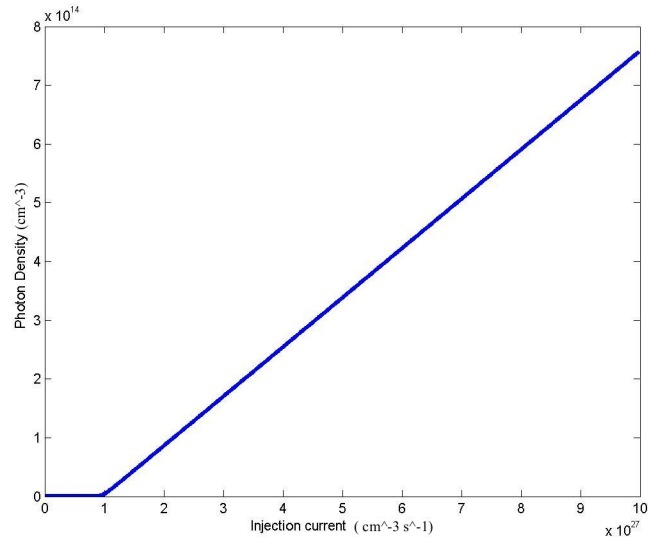


Figure 2.20: Calculated Power vs. Current (LI) Curve

laser.

## 2.5.2 Modulation

Current modulation of a laser occurs when the injection current varies with time, typically as either a sinusoidal or square wave. The modulation is normally characterized by its frequency and amplitude. Typical modulation frequencies for telecommunications are 1-20GHz.

With a small signal sinusoidal injection current of the form

$$I(t) = I_{DC} + I_{AC} \sin(\omega t), \quad (2.16)$$

where  $\omega$  is the frequency of the modulation,  $I_{DC}$  is the DC input and  $I_{AC}$  is the amplitude of the AC input, the solutions of the steady-state rate equations,

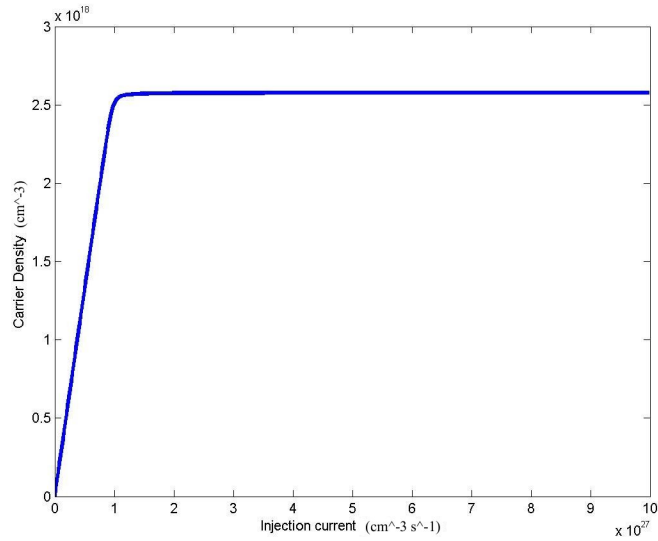


Figure 2.21: Calculated Voltage vs. Current (VI) Curve

for a small signal approximation, are of the form

$$N(t) = N_{DC} + N_{AC} \sin(\omega t) \quad (2.17)$$

$$P(t) = P_{DC} + P_{AC} \sin(\omega t) \quad (2.18)$$

with the same frequency of oscillation as the injection current. Figure 2.22 shows the output of injection current versus time for the MATLAB simulation of the steady-state rate equations. Figure 2.23 and Figure 2.24 show the calculated the photon density versus time curve and carrier density versus time curve, respectively, generated by the same MATLAB simulation with the sinusoidal injection current.

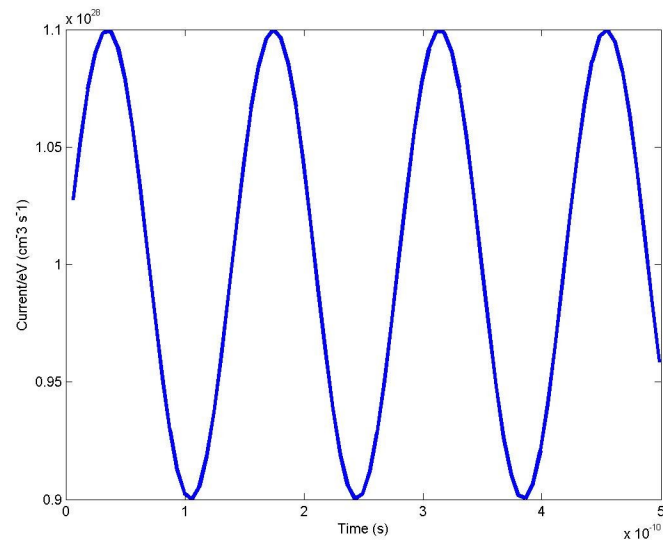


Figure 2.22: Sinusoidal Injection Current versus Time for  $f = 2\text{GHz}$

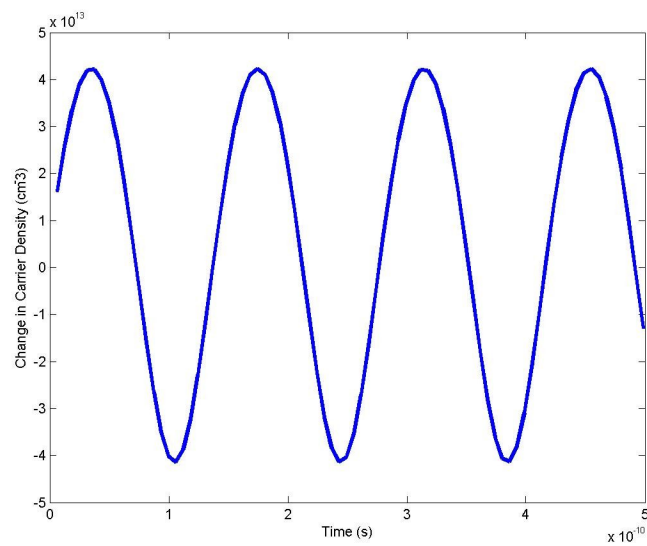


Figure 2.23: Solution for Carrier Density with a Sinusoidal Injection Current for  $f = 2\text{GHz}$

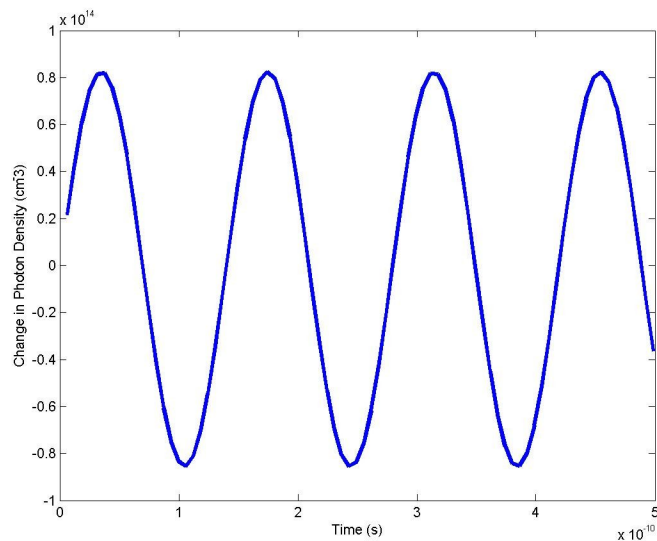


Figure 2.24: Solution for Photon Density with a Sinusoidal Injection Current for  $f= 2\text{GHz}$

## 2.6 VCSEL Fundamentals

The structure of a vertical-cavity surface-emitting laser (VCSEL) only bears a passing resemblance to the commonly envisioned laser portrayed by popular science fiction, or used in laser shows and laser pointers. The first obvious difference between these iconic images and a VCSEL is size. A typical VCSEL has a height on the order of a few microns and a diameter on the order of a 100 microns or less. To give the reader a proper sense of scale, a human hair is on average between 50 - 100 microns in diameter. The height of the VCSEL plays an important role in determining the lasing frequency of the VCSEL.

The second major discrepancy between the common conception of a laser

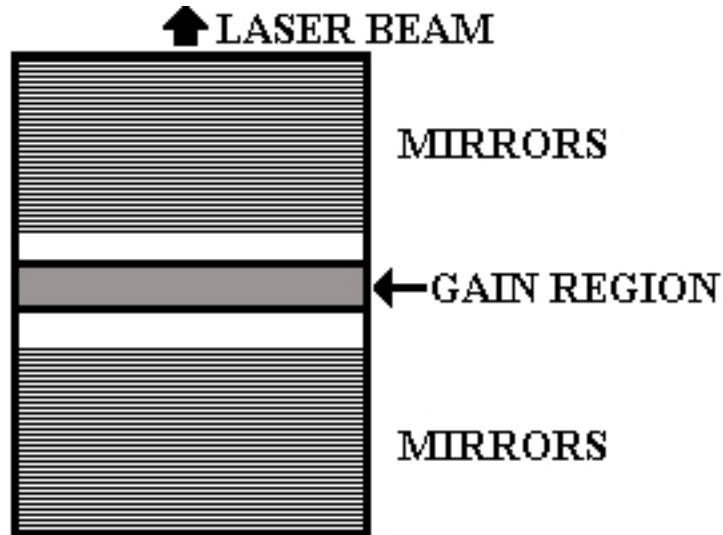


Figure 2.25: VCSEL Structure

and a VCSEL is the structure of the mirrors. Mirrors are generally imagined as panes of silvered glass. However, a mirror can be any material that will reflect light at the material junction. The mirrors of a VCSEL are actually one of the most complicated and ingenious parts of the VCSEL. They are complicated enough to warrant an entire section devoted to their design.

Figure 2.25 shows the general structure of a VCSEL.

### 2.6.1 VCSEL Lasing Frequency

VCSELs only have one Fabry-Perot frequency that falls inside the gain spectrum. This is because the cavity length,  $L$ , for a VCSEL is very small, on the order of a couple microns. So, the distance between frequencies,  $\Delta f = \frac{cn}{2L}$

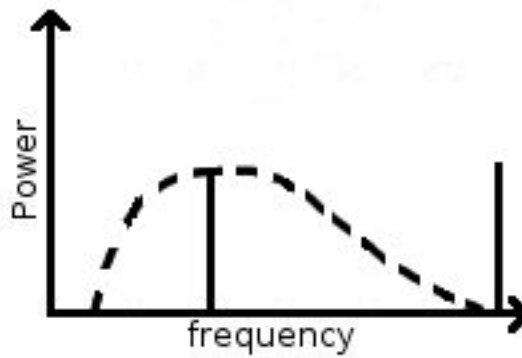


Figure 2.26: VCSEL Lasing Frequency

becomes very large. The distance between frequencies is large enough that VCSELs must be designed very carefully for any Fabry-Perot frequencies to fall inside the gain spectrum, as shown in Figure 2.26.

So, VCSELs can only lase in one longitudinal mode.

## 2.6.2 Bragg Mirrors

Index of refraction differences between the layers in a set of mirrors are responsible for the mirrors reflectivity.

The light that ends up circulating in a laser is transverse electrically (TE) polarized and transverse magnetically (TM) polarized and intersects the mirrors at normal incidence. Any light not at normal incidence to the mirrors will eventually be reflected out the sides of the laser. Thus, the light at the boundary looks like Figure 2.27.

The field reflectivity,  $r$ , and the field transmittivity,  $t$ , of the incident TE

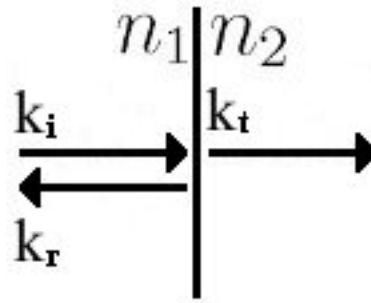


Figure 2.27: Reflection from a boundary

wave,  $\mathbf{E}_i$ , are defined as

$$r \equiv \frac{\mathbf{E}_r}{\mathbf{E}_i} \quad (2.19)$$

$$t \equiv \frac{\mathbf{E}_t}{\mathbf{E}_i} \quad (2.20)$$

where  $\mathbf{E}_r$  is the reflected wave and  $\mathbf{E}_t$  is the transmitted wave. Experimentally, we discuss the power of the wave instead of the electric field. The power of an electromagnetic wave is proportional to  $P \sim |E|^2$ . The power reflectivity  $R$  and power transmittivity  $T$  at normal incidence are then defined as ([12])

$$R \equiv \frac{P_r}{P_i} = \frac{|E_r|^2}{|E_i|^2} = r^2 \quad (2.21)$$

$$T \equiv \frac{P_t}{P_i} = \frac{|E_t|^2}{|E_i|^2} = t^2 \quad (2.22)$$

where  $P_r$  is the reflected power and  $P_t$  is the transmitted power. Conservation of energy dictates

$$R + T = r^2 + t^2 = 1. \quad (2.23)$$

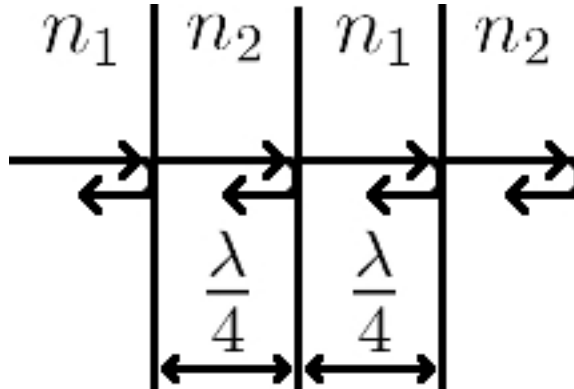


Figure 2.28: Bragg Mirror Layers

For a normal incidence TE and TM polarized waves, the field reflectivity is known to be ([12])

$$r = \frac{n_1 - n_2}{n_1 + n_2}. \quad (2.24)$$

If  $r > 0$  then the reflected wave experiences no phase shift. If  $r < 0$ , then the reflected wave experiences a phase shift of  $\pi$ .

The mirror of a VCSEL is constructed from 30-40 mirror pairs, layers of materials of indices of refraction  $n_1$  and  $n_2$  (Figure 2.28), where each layer has a thickness of  $\lambda_m/4$  where  $\lambda_m = \frac{\lambda}{n_m}$  is the lasing wavelength of the VCSEL in some material with index of refraction  $n_m$  and  $\lambda$  is the lasing wavelength in a vacuum. These layers have been designed such that all reflected light interferes constructively with the incident light. This is shown below for two propagation path cases, where the light travels from a layer with index of refraction  $n_1$  and is either reflected at a mirror layer with index of refraction  $n_1$  or  $n_2$ .

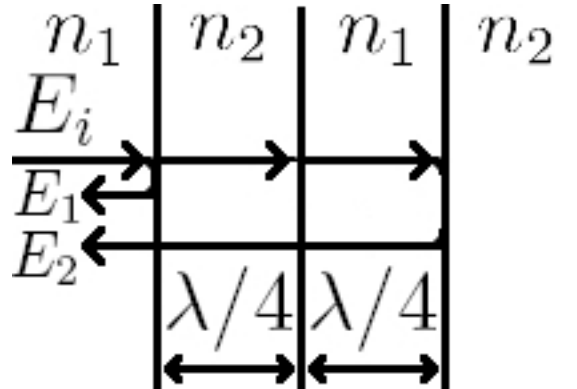


Figure 2.29: Light Paths for Case 1

Case 1: Let  $n_1 > n_2$  and the light from the incident wave,  $\mathbf{E}_i = E_i e^{i\phi}$ , travel the path shown in Figure 2.29, where  $E_1$  is the reflected light from the first boundary, and  $E_2$  is the reflected light from the third boundary. Let  $r_{jm}$  and  $t_{jm}$  denote the reflectivity and transmittivity respectively for a wave traveling from a material with index of refraction  $n_j$  to a material with index of refraction  $n_m$ .

At the first boundary,  $E_1$  acquires no phase change during this reflection because  $n_1 > n_2$  and thus

$$r = \frac{n_1 - n_2}{n_1 + n_2} > 0, \quad (2.25)$$

Since  $E_1$  only reflects from the first boundary,

$$E_1 = r_{12} E_i. \quad (2.26)$$

$E_2$  is transmitted through the first and second boundaries it is incident with. Each transmission through a boundary decreases the amplitude of the

wave by a factor  $t_{jm}$  and each propagation distance through a mirror layer with index of refraction  $n_m$  causes a change in phase  $e^{ik_m \frac{\text{lambda}_m}{4}}$ , where  $k_m = \frac{2\pi}{\lambda_m}$  is the wave number of the light  $E_2$  is reflected at the third boundary, again  $n_1 > n_2$  and no phase change occurs. Then, the light is transmitted back through the previous boundaries to the initial mirror layer. The final amplitude of  $E_2$  is

$$E_2 = E_i \underbrace{t_{12}}_{\text{boundary1}} e^{ik_2 \frac{\lambda_2}{4}} \underbrace{t_{21}}_{\text{boundary2}} e^{ik_1 \frac{\lambda_1}{4}} \underbrace{r_{12}}_{\text{boundary3}} \quad (2.27)$$

$$* \underbrace{t_{12}}_{\text{boundary2}} e^{ik_1 \frac{\lambda_1}{4}} \underbrace{t_{21}}_{\text{boundary1}} e^{ik_2 \frac{\lambda_2}{4}} \quad (2.28)$$

$$= E_i t_{12}^2 t_{21}^2 r_{12} \quad (2.29)$$

Since neither  $E_1$  nor  $E_2$  have a net phase shift, then  $E_i$ ,  $E_1$ , and  $E_2$  are in phase.

Case 2: In this case,  $E_2$  is reflected from the second boundary instead of the third, where  $n_2 > n_1$ , as shown in Figure 2.30. At the second boundary  $r < 0$ , so  $E_2$  will acquire a phase change of  $\pi$  at that boundary. Then,

$$E_2 = E_i \underbrace{t_{12}}_{\text{boundary1}} e^{ik_2 \frac{\text{lambda}_2}{4}} \underbrace{r_{21} e^{i\pi}}_{\text{boundary2}} \underbrace{t_{21}}_{\text{boundary1}} e^{ik_2 \frac{\text{lambda}_2}{4}} \quad (2.30)$$

$$= E_i t_{12} t_{21} r_{21} e^{i(2k_2 \frac{\lambda_2}{4} + \pi)} \quad (2.31)$$

$$= E_i t_{12} t_{21} r_{21} e^{i(\frac{2\pi}{\lambda_2} \frac{\lambda_2}{2} + \pi)} \quad (2.32)$$

$$= E_i t_{12} t_{21} r_{21} \quad (2.33)$$

Therefore,  $E_2$ ,  $E_1$  and  $E_i$  are in phase in this case too.

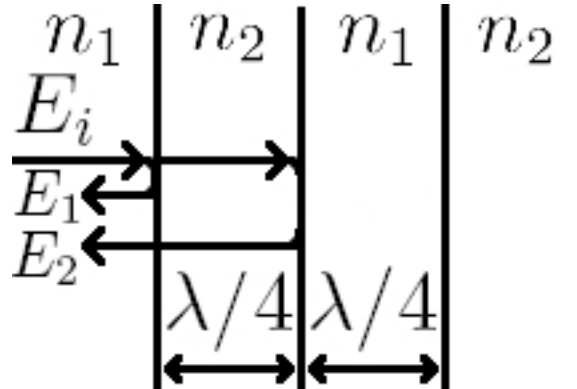


Figure 2.30: Light Paths for Case 2

Any propagation path of light through the mirror layers of the laser conforms to the same circumstances as the previous two cases. If the light reflects off a boundary and there is no phase change from the reflection, then the zero net phase change over the course of the trip is due entirely to the distance of propagation through the various mirror layers. If the light reflects off a boundary and acquires a phase change of  $\pi$ , then the distance of propagation is such that even with a phase change from the boundary there is no net phase change of the light over the course of the trip. Thus, all light in the laser is in phase and interferes constructively with the circulating light in the gain region.

## 2.7 Polarization

In addition to the spectral characteristics typical of all lasers, a VCSEL's light is linearly polarized in one of two orthogonal polarizations, where each polarization is parallel to one of the axes of the material lattice structure of the VCSEL. Most VCSELs have a characteristic current at which the laser switches from one polarization to the other. This switching current is dependent upon the initial polarization of the light. If the laser has some X polarization and switched to a Y polarization, then the magnitude of the switching current will be different than if the laser was switching from the Y polarization to the X polarization. Thus, the switching current has some inherent hysteresis.

## 2.8 Conclusion

This chapter has derived many of the spectral characteristic of semiconductor lasers in general and VCSELs in particular, such as the lasing frequency, threshold current, laser output power, power modulation due to a modulated injection current, laser coherence, and laser polarization. These are the VCSEL characteristics that will be the focus of the proceeding chapters and experiment.

## Chapter 3

# FEEDBACK

Extremely-short external-cavity feedback occurs when light is back-reflected into the laser from a reflective surface a few tens of microns from the aperture of the laser. For a VCSEL this is well within the coherence length, which is on the order of 1cm, so the back-reflected light still bears a strong phase relationship to the light in the lasing cavity. Since the back-reflected light still has a well defined phase relation to the lasing emission, the feedback can be modeled as light in a three cavity system, as shown in Figure 3.2. Using a derivation based on the three cavity model, the original rate equations for a laser will be modified to include the effects of ESEC feedback.

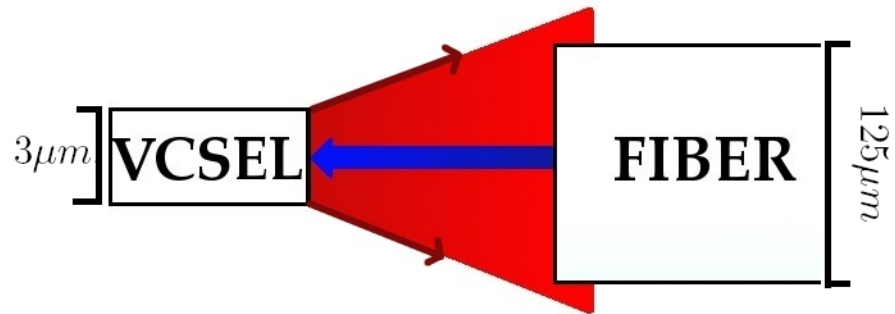


Figure 3.1: Feedback from a Fiber to a VCSEL

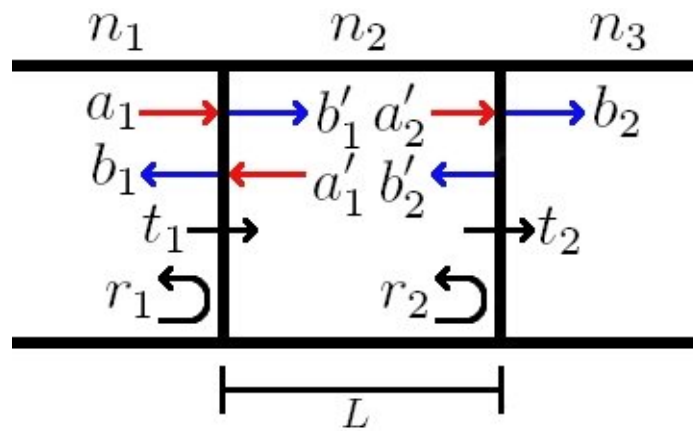


Figure 3.2: Three Cavity System

### 3.1 Derivation

In this experiment, the external feedback comes from an optical fiber positioned within tens of microns of the VCSEL, as estimated by a grating in the one eyepiece of the microscope, with the face of the fiber parallel to the aperture of the VCSEL. A portion of the light from the VCSEL is reflected at the face of the fiber, while the rest of the light is transmitted through the fiber to the detection system at the other end of the fiber. The reflection of light at the fiber face is due to the index of refraction change between the air and the glass of the fiber. This system is shown in Figure 3.1, where the blue arrow pointing from the fiber to the laser represents the back-reflected light.

The three cavity system shown in Figure 3.2 represents the VCSEL-air-fiber system, where the leftmost material, material 1, represents the VCSEL material, the rightmost material, material 3, represents an optical fiber, and the central material, material 2, is the air between the two, also known as the external cavity. Similarly, index of refraction  $n_1$  is the index of refraction of the VCSEL,  $n_2$  is the index of refraction of air, and  $n_3$  is the index of refraction of the fiber. Arrows have been drawn to represent the light entering and leaving the boundaries between materials. The arrows pointing toward a boundary, the red arrows, are light entering the boundary, while the arrows pointing away from the boundary, the blue arrows, are light leaving the boundary. Since the optical fiber is not a source of light there is no light entering the

$n_2/n_3$  boundary, denoted from now on as boundary 2/3, from the right.

The reflectivity of the  $n_1/n_2$  boundary, denoted from now on as boundary 1/2, from the left is  $+r_1$ . The reflectivity of boundary 1/2 from the right is  $-r_1$ . The transmittivity of boundary 1/2 is positive for light transmitted from material 1 to material 2. The same convention holds from boundary 2/3; the reflectivity has a positive sign for light incident from the left and the transmittivity has a positive sign for light transmitted from material 2 to material 3, where the sign just indicates the direction of approach. Whether or not the reflectivity is inherently positive or negative comes from Eqn.2.24. The equations for the light at boundary 1/2 are:

$$b_1 = a_1 r_1 + a'_1 t_1 \quad (3.1)$$

$$b'_1 = a_1 t_1 - a'_1 r_1 \quad (3.2)$$

where  $a_1$ ,  $b_1$ ,  $a'_1$  and  $b'_1$  are the amplitudes of the electric fields of the light.

The equations for the light at boundary 2/3 are:

$$b_2 = a'_2 t_2 \quad (3.3)$$

$$b'_2 = a'_2 r_2 \quad (3.4)$$

The equations for the light displacement as it travels through material 2 are:

$$a'_1 = b'_2 e^{-i\beta L} \quad (3.5)$$

$$a'_2 = b'_1 e^{-i\beta L} \quad (3.6)$$

where  $\beta_2 = \frac{2\pi}{\lambda_2}$  is the wavenumber of the light,  $\lambda_2 = \frac{\lambda}{n_2}$  is the wavelength of the light in material 2,  $\lambda$  is the lasing wavelength in a vacuum, and  $L$  is the length of the external cavity, the distance light travels [4]. Since material 2 is the air between the laser and the fiber, then  $n_2 \approx 1$  and  $\beta_2 = \frac{2\pi n_2}{\lambda} \approx \frac{2\pi}{\lambda}$ .

Feedback depends on the amount of light from the external cavity that is back reflected into the laser by the fiber. A portion of the back-reflected light is transmitted into the lasing cavity, while the remaining light is reflected at the output laser mirror. In Figure 3.2, the total light reflected back into the lasing cavity is

$$b_1 = a_1 r_1 + a'_1 t_1 \quad (3.7)$$

where  $a_1$  is light reflected at the output laser mirror and  $a'_1$  is light originally reflected at the fiber.

The characteristics of the laser beam depend on the light in the laser, some initial amount of light plus  $b_1$ . The role of the external cavity is to change the amount of light back reflected into the laser and accomplishes this by introducing an amount of light  $a'_1 t_1$  into the laser cavity. Thus, the external cavity changes the total amount of light in the lasing cavity. This change in the total amount of light due to a contribution from the external cavity can be modeled as a change in the reflectivity of the mirror of the laser, boundary 1/2. The following derivation mimics the model originally derived in [4].

The laser and external cavity system can be approximated as the laser

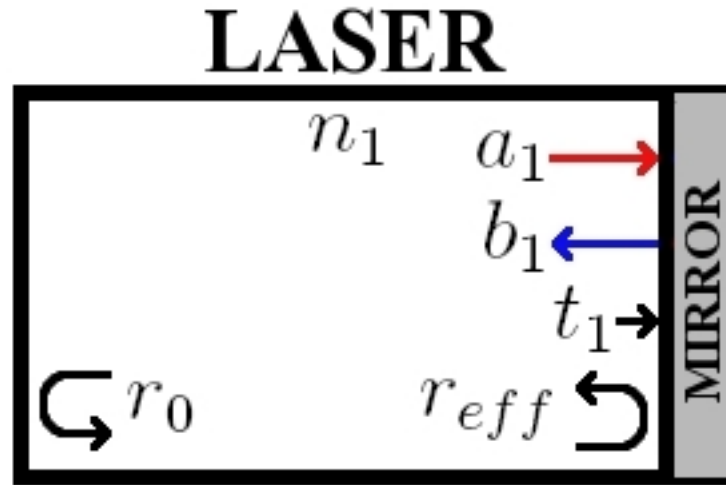


Figure 3.3: Laser with Effective Mirror

with the effective reflectivity for one of the mirrors, as shown in Figure 3.3, where  $r_0$  is the reflectivity of the other laser mirror. The total reflected light at the output mirror is still  $b_1$ , but now

$$b_1 = a_1 r_{eff} \quad (3.8)$$

The reflectivity of a boundary is defined as the ratio of the light reflected from a boundary to the light incident on the boundary. Solving the previous boundary equations ([4]) for  $a_1$  and  $b_1$ , the new effective reflectivity,  $r_{eff}$  of boundary 1/2 is

$$r_{eff} = \frac{b_1}{a_1} = r_1 + \frac{t_1^2 r_2 e^{-2i\beta_2 L}}{1 + r_1 r_2 e^{-2i\beta_2 L}} \quad (3.9)$$

If the feedback from the external cavity reflector is weak, then  $r_2$  is small.

Then,

$$1 + r_1 r_2 e^{-2i\beta_2 L} \approx 1 \quad (3.10)$$

and

$$r_{eff} \approx r_1 + t_1^2 r_2 e^{-2i\beta_2 L} \quad (3.11)$$

$$= r_1 + t_1^2 r_2 (\cos(2\beta_2 L) - i \sin(2\beta_2 L)). \quad (3.12)$$

The effective reflectivity can also be written as

$$r_{eff} = r_1 + \Delta r. \quad (3.13)$$

If  $\Delta r_R$  is the real term of the change in reflectivity and  $\Delta r_i$  is the imaginary term of the change in reflectivity, then the magnitude of the effective reflectivity is

$$|r_{eff}|^2 = r_{eff} r_{eff}^* \quad (3.14)$$

$$= ((r_1 + \Delta r_R) + i\Delta r_i)((r_1 + \Delta r_R) - i\Delta r_i) \quad (3.15)$$

$$= (r_1 + \Delta r_R)^2 + \Delta r_i^2 \quad (3.16)$$

$$= (r_1 + \Delta r_R)^2 + t_1^4 r_2^2 \sin^2(2\beta_2 L). \quad (3.17)$$

Since the imaginary term  $\Delta r_i$  depends on  $r_2^2$  and  $r_2$  is small, then the term can be neglected. So,

$$|r_{eff}| \approx r_1 + \Delta r_R \quad (3.18)$$

$$= r_1 + t_1^2 r_2 \cos(2\beta_2 L). \quad (3.19)$$

This new reflectivity changes the fraction of light lost from the laser and, by extension, the average amount of time the photons stay in the laser, defined as the photon lifetime. Before the external cavity was added, the total loss term for a round trip of light through the lasing cavity was defined as ([4])

$$\alpha = \alpha_i + \alpha_m, \quad (3.20)$$

where  $\alpha_i$  is the internal loss, or the loss per unit length due to scattering and absorption inside the cavity, and  $\alpha_m$  is the spatially averaged contribution to the loss from the both mirrors.

For an initial light wave  $E = E_o e^{i\phi}$ , the loss from both mirrors in the laser is written as

$$E_o e^{i\phi} e^{-2L_c \alpha_m} = R_o R_1 E_o e^{i\phi} \quad (3.21)$$

where  $e^{-2L_c \alpha_m}$  is the total fraction of light lost due to reflection from both mirrors for one round trip through the lasing cavity, a trip of distance  $2L_c$ , twice the length of the lasing cavity. Thus, the mirror loss term is defined as

$$\alpha_m = \frac{1}{L_c} \ln\left[\frac{1}{R}\right] = \frac{1}{L_c} \ln\left[\frac{1}{r_0 r_1}\right]. \quad (3.22)$$

The total loss for any distance light travels in inside the laser is then

$$loss = x * \alpha \quad (3.23)$$

where  $x$  is some distance traveled. The instantaneous rate of photon loss is the derivative of the loss with respect to time. Since  $\alpha$  is a constant, then the

rate of photon loss is

$$\frac{d(loss)}{dt} = \frac{d}{dt}(x\alpha) = \alpha v. \quad (3.24)$$

Then the average rate of photon loss per unit time is  $\alpha v_{avg} = \alpha v_g$ . The photon lifetime, the average amount of time a photon spends in the cavity, is then ([4])

$$\tau_p = \frac{1}{v_g \alpha} = \frac{1}{v_g(\alpha_i + \alpha_m)}. \quad (3.25)$$

The equation of light for an initial wave  $E = E_o e^{i\phi}$  that makes one trip from one mirror to the other through the lasing cavity with the new effective mirror reflectivity  $r_{eff}$ , and the new total loss  $\alpha_{new}$ , can be written as

$$E_o e^{i\phi} e^{(2L_c)(-\alpha_{new})} = R_{eff} R_0 e^{(2L_c)(-\alpha_i)} E_o e^{i\phi} \quad (3.26)$$

$$-2\alpha_{new} L_c = \ln[R_{eff} R_0 e^{-2\alpha_i L_c}] \quad (3.27)$$

$$= -2\alpha_i L_c + \ln[R_{eff} R_0] \quad (3.28)$$

$$\alpha_{new} = \alpha_i - \frac{1}{2L_c} \ln[R_{eff} R_0] \quad (3.29)$$

$$= \alpha_i + \frac{1}{2L_c} \ln\left[\frac{1}{(r_1 + \Delta r_R)^2 r_0^2}\right] \quad (3.30)$$

$$= \alpha_i + \frac{1}{L_c} \ln\left[\frac{1}{(r_0 r_1)(1 + \frac{\Delta r_R}{r_1})}\right] \quad (3.31)$$

$$= \alpha_i + \frac{1}{L_c} \ln\left[\frac{1}{r_0 r_1}\right] + \frac{1}{L_c} \ln\left[\frac{1}{(1 + \frac{\Delta r_R}{r_1})}\right] \quad (3.32)$$

$$= \alpha_i + \frac{1}{L_c} \ln\left[\frac{1}{r_0 r_1}\right] + \frac{1}{L_c} \ln\left[\frac{r_1}{r_1 + \Delta r_R}\right] \quad (3.33)$$

$$= \alpha_i + \alpha_m + \frac{1}{L_c} \ln\left[1 - \frac{\Delta r_R}{r_1 + \Delta r_R}\right]. \quad (3.34)$$

Since  $\Delta r_R = t_1^2 r_2 \cos(2\beta_2 L)$  and  $r_2$ , the reflectivity of the fiber, is small, then  $\Delta r_R$  is also small. Thus a Taylor expansion of  $\ln[1 - \frac{\Delta r_R}{r_1 + \Delta r_R}]$  can be used

to express  $\alpha_{new}$  as

$$\alpha_{new} \approx \alpha_i + \alpha_m - \frac{\Delta r_R}{L_c(r_1 + \Delta r_R)}. \quad (3.35)$$

Also since  $r_2$  is small, much smaller than  $r_1$ , then  $\Delta r_R$  is much smaller than  $r_1$ . Thus

$$\alpha_{new} \approx \alpha_i + \alpha_m - \frac{1}{L_c} \frac{\Delta r_R}{r_1}. \quad (3.36)$$

Then, the new photon lifetime is

$$\frac{1}{\tau'_p} = v_g \alpha_{new} \quad (3.37)$$

$$= v_g \left( \alpha_i + \alpha_m - \frac{1}{L_c} \frac{\Delta r_R}{r_1} \right) \quad (3.38)$$

$$= v_g (\alpha_i + \alpha_m) - \frac{v_g}{L_c} \frac{\Delta r_R}{r_1} \quad (3.39)$$

$$= \frac{1}{\tau_p} - \frac{v_g}{L_c} \frac{\Delta r_R}{r_1} \quad (3.40)$$

$$= \frac{1}{\tau_p} - \frac{v_g t_1^2 r_2}{r_1 L_c} \cos(2\beta_2 L) \quad (3.41)$$

$$= \frac{1}{\tau_p} - 2\kappa \cos(2\beta_2 L), \quad (3.42)$$

where  $\kappa = \frac{v_g t_1^2 r_2}{2r_1 L_c} = \frac{t_1^2 r_2}{r_1 \tau_L}$  and  $\frac{1}{\tau_L} = \frac{v_g}{2L_c}$  is the time it takes for the light to make one round trip through the lasing cavity.  $\kappa$  is defined as the feedback coefficient since it determines the amplitude of the feedback effects.

Substituting the new photon lifetime term for the old photon lifetime in the photon density rate equation yields ([4])

$$\left( \frac{dP}{dt} \right)_{feedback} = v_g \frac{dg}{dN} (N - N_{tr}) P \Gamma - \frac{P}{\tau'_p} + \beta \frac{N}{\tau} \quad (3.43)$$

$$= v_g \frac{dg}{dN} (N - N_{tr}) P \Gamma + \beta \frac{N}{\tau} - P \left[ \frac{1}{\tau_p} - 2\kappa \cos(2\beta_2 L) \right] \quad (3.44)$$

$$= v_g \frac{dg}{dN} (N - N_{tr}) P \Gamma + \beta \frac{N}{\tau} - \frac{P}{\tau_p} + 2P\kappa \cos(2\beta_2 L) \quad (3.45)$$

$$= \left( \frac{dP}{dt} \right)_{old} + 2P\kappa \cos(2\beta_2 L) \quad (3.46)$$

So, the rate equations for a laser with feedback from an external cavity

are:

$$\frac{dN}{dt} = \frac{I}{eV} - \frac{N}{\tau} - v_g \frac{dg}{dN} (N - N_{tr}) P \quad (3.47)$$

$$\frac{dP}{dt} = v_g \frac{dg}{dN} (N - N_{tr}) P \Gamma + \beta \frac{N}{\tau} - \frac{P}{\tau_p} + 2P\kappa \cos(2\beta_2 L) \quad (3.48)$$

## 3.2 Steady-State Solutions with Feedback

The steady-state rate equations with feedback are then

$$0 = \frac{I}{eV} - \frac{N}{\tau} - v_g \frac{dg}{dN} (N - N_{tr}) P \quad (3.49)$$

$$0 = v_g \frac{dg}{dN} (N - N_{tr}) P \Gamma + \beta \frac{N}{\tau} - \frac{P}{\tau_p} + 2P\kappa \cos(2\beta_2 L). \quad (3.50)$$

Then the modified solutions for P and N, from Ch.2.5.1, are

$$P_{fb} = \frac{\frac{I}{eV} - \frac{N}{\tau}}{v_g \frac{dg}{dN} (N - N_{tr})} \quad (3.51)$$

$$N_{fb} = \frac{\tau}{\beta - \Gamma} \left[ \frac{P}{\tau_p} - \Gamma \frac{I}{eV} \right] \quad (3.52)$$

$$= \frac{\tau}{\beta - \Gamma} \left[ \frac{P}{\tau_p} - 2\kappa \cos(2\beta_2 L) - \Gamma \frac{I}{eV} \right] \quad (3.53)$$

$$= \frac{\tau}{\beta - \Gamma} \left[ \frac{P}{\tau_p} - \Gamma \frac{I}{eV} \right] - \frac{2\kappa\tau}{\beta - \Gamma} \cos(2\beta_2 L) \quad (3.54)$$

where N has a clear sinusoidal dependence upon L, the length of the external cavity. Modification of the corresponding MATLAB program from Ch.2.5.1

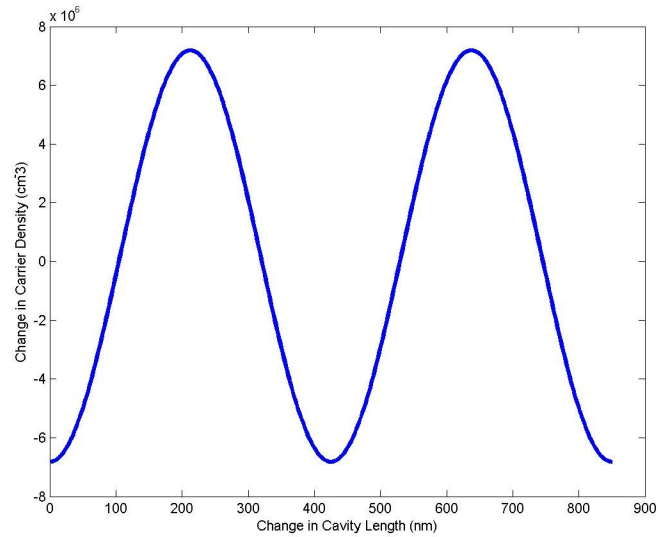


Figure 3.4: Calculated Carrier Density vs. External Cavity Length

with input values as listed in Table 2.1, yields Figure 3.4, a graph of carrier density versus change in external cavity length. Figure 3.4 confirms the sinusoidal dependence of  $N$  on  $L$  and predicts that for a laser of wavelength  $\lambda = 850nm$  and  $\beta_2 = \frac{2\pi}{\lambda}$ , the period of oscillation of  $N$  will be  $\lambda/2 = 425nm$ .

Since  $N$  has a sinusoidal dependence on  $L$ , by extension  $P$  has a sinusoidal dependence on  $L$  with the same period of oscillation, as shown in Figure 3.5. The output power of the VCSEL is proportional to its photon density. Thus, the output power should also vary sinusoidally with external cavity length and have a period of  $\lambda/2$ .

The gain of the laser is also related to the carrier density, by  $g = \frac{dg}{dN}(N - N_{tr})$ . The linear relation between  $g$  and  $N$  again suggests that gain should vary

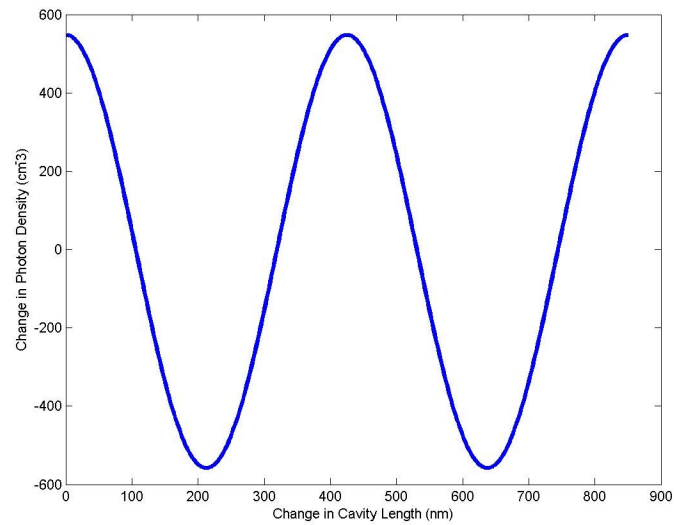


Figure 3.5: Calculated Photon Density vs. External Cavity Length

sinusoidally with a period of half the lasing wavelength and be in phase with the carrier density. Figure 3.6 shows the sinusoidal variation of the gain, the half lasing wavelength period. A comparison of Figure 3.6 and Figure 3.4 shows that gain and carrier density are in phase.

Ch.2 stated that the laser begins to lase when the gain of the lasing mode equals its loss. This equality was characterized by the threshold current, the current at which optical gain equals loss. Then a variation in the gain should result in a variation of the threshold current of the VCSEL. Since the gain varies sinusoidally with external cavity length, then the threshold current should do the same. Figure 3.7 shows a calculated shift in threshold current due to a change in the external cavity length.

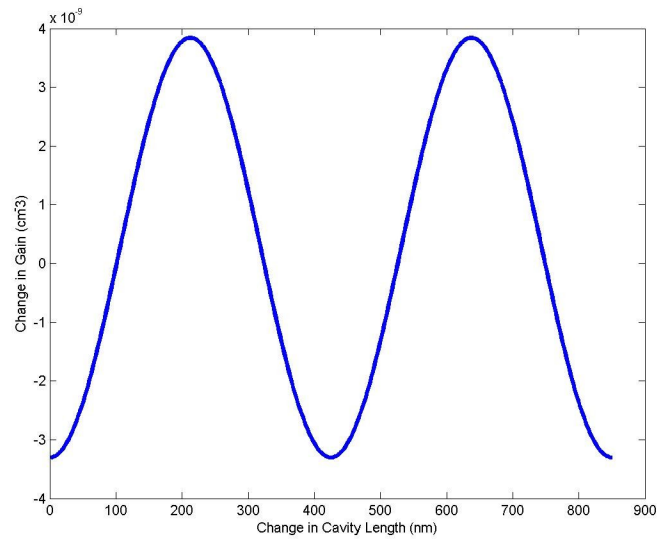


Figure 3.6: Calculated Gain vs. External Cavity Length

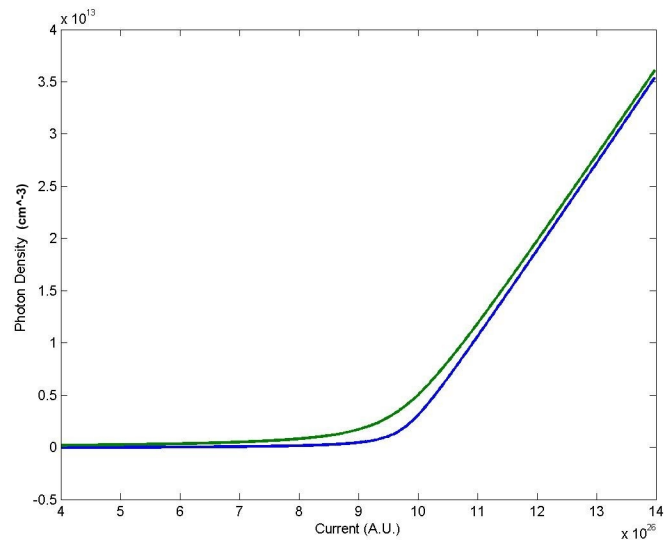


Figure 3.7: Calculated Threshold Current Shift due to Feedback

If the value of the gain at threshold is  $g_{th}$  then the threshold gain with feedback can be written as  $g_{th} = g_i + \Delta g_{fb}$ , where  $g_i$  is the gain due to the injection current and  $\Delta g_{fb}$  is the change in gain due to feedback from the external cavity. If  $\Delta g_{fb} < 0$ , then  $g_i > g_{th}$ . Thus, if the feedback causes a decrease in the gain, then a greater injection current is required for  $g = g_{th}$ . Similarly, if  $\Delta g_{fb} > 0$ , then  $g_i < g_{th}$ . Thus, if the feedback causes an increase in the gain, then less current is required to reach threshold. This results in a phase shift of  $\pi$  between the oscillations in the gain and the oscillations in the threshold current.

In addition to power and threshold current variations with feedback, lasing wavelength ([1],[13]) and polarization switching current and polarization switching current hysteresis width ([2],[14]) variations have been predicated and observed. The lasing wavelength shift is in part due to Ohmic heating, and is therefore related to the variation in power and threshold current. The period of oscillation should be the same as that of the power and threshold current, an external cavity change of half the lasing wavelength. The polarization switching current and its hysteresis width variations have been shown to also have a period of half the lasing wavelength.

The half lasing wavelength period of oscillation for all the output beam characteristics makes intuitive sense from the perspective of interference. If the back-reflected light is  $\pi$  out of phase with the light in the lasing cavity, then

the back-reflected light interferes destructively with the light in the cavity. The destructive interference is effectively another form of loss in the lasing cavity. Therefore, the total gain in the lasing cavity decreases when the back-reflected light is  $\pi$  out of phase with the light in the cavity. Similarly, if the back-reflected light is in phase with the light in the lasing cavity, then the back-reflected light interferes constructively with the light in the lasing cavity. Thus, the total gain increases when the back-reflected light that is in phase with the light in the lasing cavity.

### 3.3 Summary

The laser rate equations with an additional term due to feedback from an external cavity predict a cosine dependence of the threshold current and power of the laser on the external cavity length. In addition, the same sinusoidal dependence on external cavity length has been predicted for the lasing wavelength, the polarization switching current, and the hysteresis width of the polarization switching current. The period of oscillation for all the laser characteristics is half the lasing wavelength.

## Chapter 4

# Experiment

This experiment was designed to mimic an instance in industry where ESEC feedback into a modulated VCSEL would actually occur: when an optical fiber is butt-coupled to a VCSEL in a telecommunications network.

The core of the experiment is a single-mode optical fiber and a 850nm VCSEL. The fiber has been stripped of all packaging and cladding and cleaved to create a reflective surface. Similarly, the canister packing of the VCSEL has been removed to allow for close proximity of the fiber facet and the VCSEL. The fiber is then held with the reflective facet within tens of microns of the aperture of the VCSEL. The fiber is oriented such that the facet is nominally at  $90^\circ$  to the VCSEL's output beam and light will reflect off the facet and back into VCSEL. Then, the distance between the fiber and VCSEL is varied in increments until the total change in distance is at least half the wavelength

of the VCSEL, in this case 425nm. As the distance varies, various properties of the light transferred through the fiber are measured and used to analyze characteristics of the laser. This experiment focuses on the variation with high-speed modulation and ESEC feedback of the VCSEL's threshold current, power, lasing wavelength, and polarization switching current and polarization switching current hysteresis width.

## 4.1 Experimental setup

The VCSEL for this experiment is a singlemode, oxide-confined, 850nm VCSEL. The heat sink temperature of the VCSEL is kept constant at 20° F by a thermoelectric cooler. A DC electrical bias to the VCSEL is supplied by a precision laser diode current source and an AC electrical bias is supplied by a waveform generator. The upper limit of the VCSEL modulation frequency in the experiment comes from the VCSEL itself; above 3 GHz the VCSEL power decreases rapidly until no output signal can be detected. The laser mount and heat sink are custom made, with the upper limit of the modulation frequency of the laser mount greater than the modulation frequency upper limit of the VCSEL.

The cleaved fiber is held on a fiber mount attached to a series of positioning stages: an XY stage with centimeter resolution for large initial adjustments, and an XYZ stage and a 3-direction rotational stage, both with

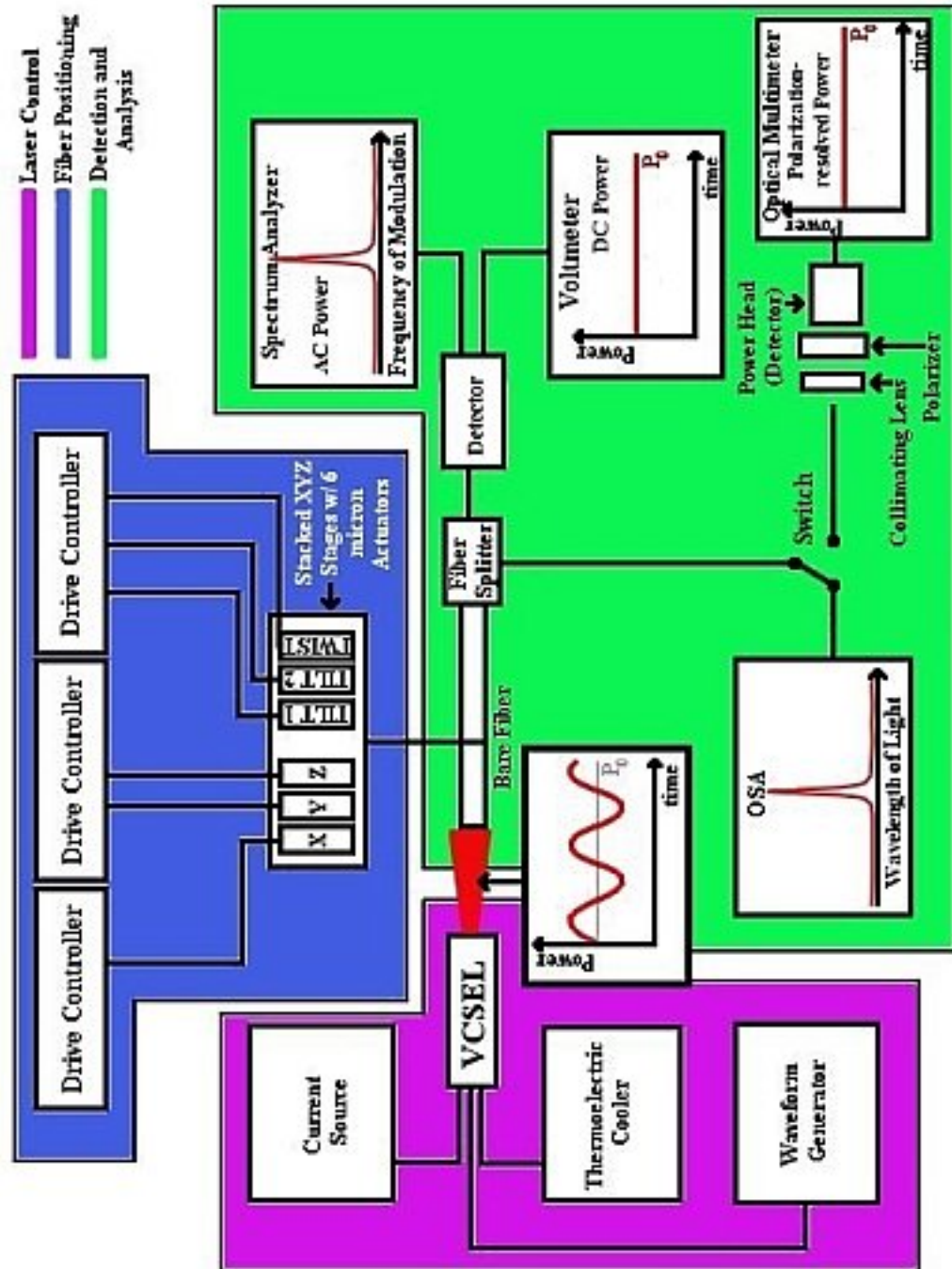


Figure 4.1: Experimental Setup: The laser control section of the setup controls the temperature and injection current of the VCSEL. The fiber positioning section adjusts the fiber facet until it is aligned normal to the laser beam. The detection and analysis section records measurements of the properties of the output beam, such as power, modulation frequency, lasing wavelength, and polarized power. Table 4.1 is a list of the equipment.

Actuators	( Tilt 1, Tilt 2, Y, Z) Newport AD-100  (Twist, X) Newport AD-40
Collimating Lens	Newport M-10X 0.25 Microscope Objective
Current Source	ILX Lightwave LDX-3210  Precision Laser Diode Current Source
Detector	Newport D-30 30ps 400-1700nm Detector
Drive Controller	Newport ESA-C $\mu$ Drive Controller
Fiber Splitter	Thorlabs 50/50 singlemode 2 by 2 850nm
Optical Multimeter	ILX Lightwave OMM-6810B Optical Multimeter
OSA	Agilent 86140B Optical Spectrum Analyzer
Polarizer	850 nm
Power Head	ILX Lightwave OMH-6703B Silicon Power Head
Spectrum Analyzer	Anritsu MS710C Spectrum Analyzer
Thermoelectric Cooler	ILX Lightwave LDT-5910B Temperature Controller
VCSEL	Advanced Optical Components SV3639-001  singlemode oxide-confined 850nm
Voltmeter	Keithly 197A Autoranging Microvolt DMM
Waveform Generator	Agilent 83712B 10MHz - 20GHz Synthesized CW Generator

Table 4.1: Equipment List corresponding to Figure 4.1

micron resolution actuators for finer adjustments. The micron actuators are controlled with Newport micron drive controllers. In this experiment, the X direction indicates the axis of the external cavity between the VCSEL and the fiber.

The output end of the fiber is connected to one input of an approximately 50/50 single mode, 850nm, 2 by 2, fiber coupler. The laser beam is coupled into one of the 2 input arms of the 2 by 2 fiber coupler and the fiber coupler splits the light evenly, but with some loss, between the 2 output arms of the coupler. One output of the coupler goes to a Newport D-30 detector which then converts the input light signal into an output voltage signal. The detector then sends the DC voltage signal, corresponding to the DC light signal, to a voltmeter and sends the AC signal to a spectrum analyzer. The voltmeter records the DC power of the VCSEL, while the spectrum analyzer records the modulation frequency of the output power. The other output of the fiber coupler goes to either an optical spectrum analyzer, which records the lasing wavelength of the VCSEL, or is directed through a collimating lens and a polarizer to a detector attached to an optical multimeter. The output of the voltmeter is used to measure the overall power signal, while the optical multimeter output is the polarized power.

The voltmeter, optical multimeter, optical spectrum analyzer and current source all have GPIB connections to a lab computer and are controlled

using LabView programs.

## 4.2 Experiment

Initially, the experiment was run with a no polarization information and a current modulation frequency of 40 MHz, the upper limit allowed by the laser mount, due to the frequency responses to the AC input of the mount components. A new mount was fabricated for higher frequency modulation and the VCSEL became the frequency limiting factor. After the new laser mount was installed, the fiber coupler and polarization setup were added to the experiment.

Then the width of the lasing spectrum of the VCSEL was examined over the accessible range of modulation frequencies for any noticeable deviations from the lasing spectrum without modulation. The spectral width of the VCSEL increased steadily until the VCSEL's upper frequency limit was reached. The maximum width occurred at 2.6 GHz. Frequencies higher than 2.6 GHz resulted in a sharp decrease in the output power of the VCSEL. The rest of the experiment was done with a current modulation frequency of 2.6 GHz, because that resulted in the largest deviation from the lasing spectrum without modulation.

The fiber was positioned to achieve maximum coupling between the VCSEL and the fiber, with the fiber as close to the VCSEL as possible without

contact. The fiber was initially adjusted on the Y and Z axes at a distance until the laser beam was located. Then the distance between the VCSEL and fiber was decreased in increments, where at every increment the coupling of the VCSEL and fiber was refined along the Y and Z axes. When the fiber was at the minimum possible distance from the VCSEL, then rotational adjustments were made to the fiber to account for the possibility that the VCSEL aperture and fiber facet were not quite parallel and thus light reflected at the fiber facet would not be directed back towards the VCSEL. Care had to be taken that maximum coupling at this cavity length was between the fiber and the center of the laser beam, as opposed to interference fringes created by the light passing through the VCSEL aperture.

Once maximum coupling for the final external cavity length was achieved, then Power versus currents curves were taken for both the total output power and the polarized output power. Next, the modulated current is applied in addition to the DC signal and the power versus current curves are taken again. Then, the external cavity length is changed and power versus current curves are taken for the new position. From these curves, threshold current, total power at a fixed current, and polarization switching current are determined.

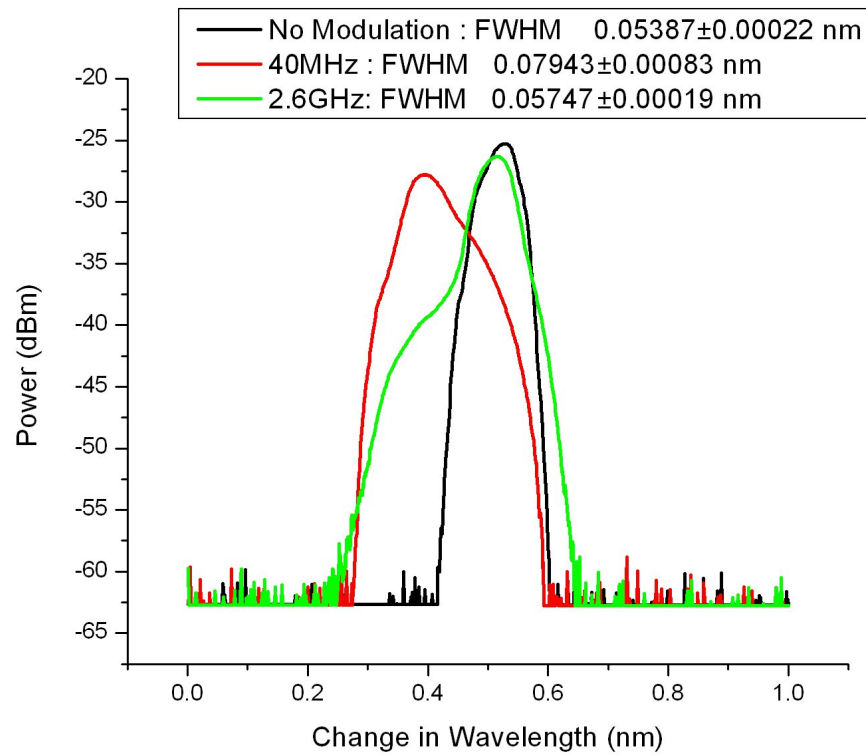


Figure 4.2: Comparison of the Spectral Width of the VCSEL for no modulation, 40MHz, and 2.6GHz

### 4.3 Coherence Length

The coherence time of the laser is effectively inversely proportional to the width of the lasing spectrum [15]. Thus, if the lasing spectrum broadens, then the coherence time decreases. As stated in Ch.2, the coherence length of the laser is given by  $l_c = c\tau_c$ , where  $l_c$  is the coherence length and  $\tau_c$  is the coherence time. If  $\tau_c$  decreases, then  $l_c$  decreases correspondingly.

Figure 4.2 compares the lasing frequency spectra for the VCSEL with

no modulation to that with modulation at 40MHz and 2.6GHz. The spectral width of the VCSEL increases with a 40MHz modulation from approximately .21 nm to .275 nm, with an increase of the full-width half-maximum of the curve from approximately .054 nm to .08 nm. A further increase of the modulation frequency to 2.6GHz increases the spectral width to approximately .3 nm and changes the FWHM to approximately .058 nm.

The increase in spectral width with current modulation indicates a decrease in the coherence length of the VCSEL. As the coherence length decreases so should the overall coherence of the back-reflected light. Thus, the feedback into the VCSEL is expected to bear a weaker phase relationship to the light in the VCSEL as the current is modulated. This suggests that the effects of ESEC feedback into a VCSEL should decrease with modulation of the VCSEL.

## 4.4 Polarization

The other VCSEL characteristic that changes noticeably with modulation is the polarization of the laser beam. The polarization of the laser beam was examined with and without modulation, in order to confirm the assertion from [9] that modulation breaks down the polarization exclusivity of the laser beam. Figure 4.3 shows the LI curves of the individual polarizations of the VCSEL without any current modulation. X denotes the polarization for currents

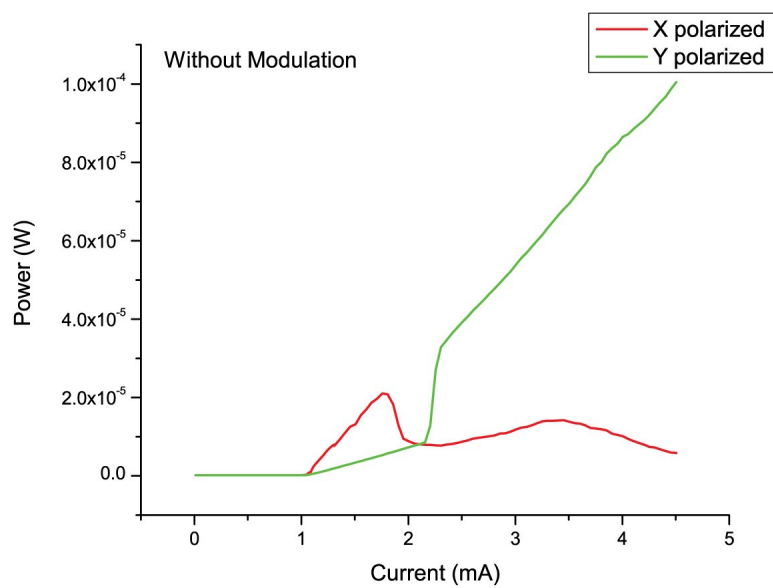


Figure 4.3: LI curves for the X and Y polarizations of a VCSEL

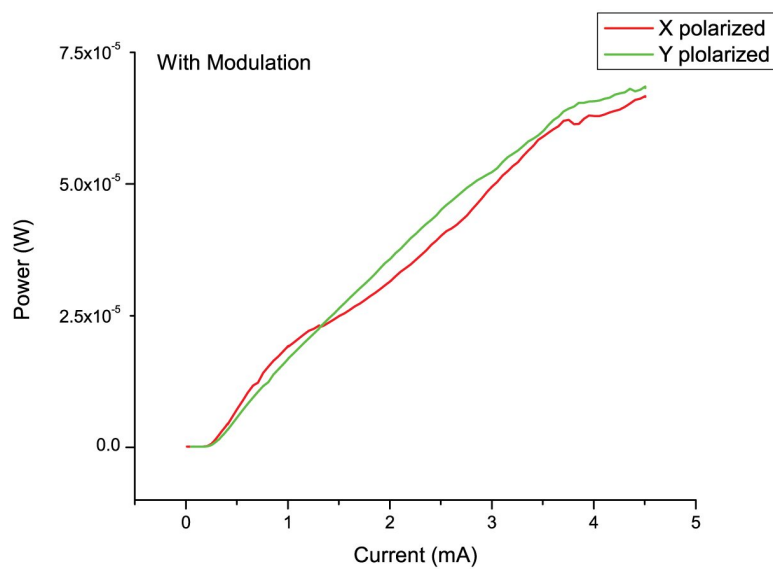


Figure 4.4: LI curves for the X and Y polarizations of a VCSEL with modulation

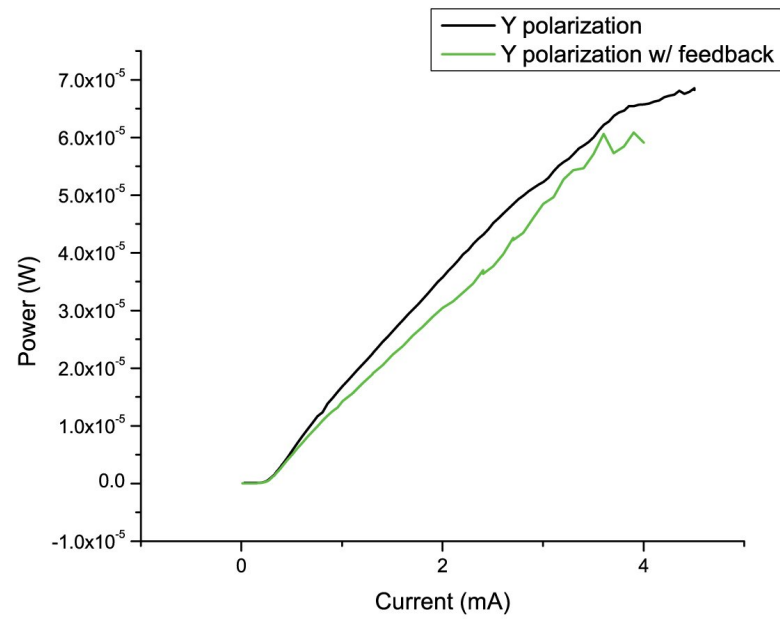


Figure 4.5: LI curves for the Y polarization of a VCSEL with and without feedback

smaller than the polarization switching current and Y denotes the polarization for currents greater than the polarization switching current. In the case without modulation, a clear polarization switch occurs at approximately 2.1 mA; the X polarization undergoes an abrupt decrease while the Y polarization increases sharply.

Figure 4.4 shows the LI curves of the X and Y polarization for the same laser, without any changes to the previous experimental parameters except for the addition of a modulation current to the VCSEL. With current modulation, there is no abrupt polarization switching. Instead, both polarizations lase simultaneously with approximately equal output powers. Since there is no polarization selectivity in the VCSEL with current modulation, this suggests that the addition of optical feedback will not be able to induce polarization switching.

Figure 4.5 compares with and without feedback cases of the LI curves of the Y polarization of the VCSEL in the presence of a modulation current. With the addition of feedback, no significant change in the VCSEL behavior is apparent, implying that feedback does not effect the polarization properties of the VCSEL with current modulation.

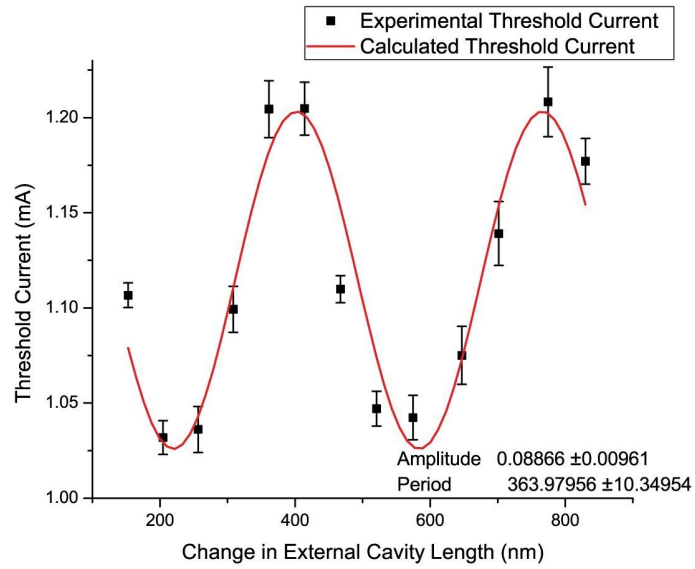


Figure 4.6: Variation of the Threshold Current with changing External Cavity Length

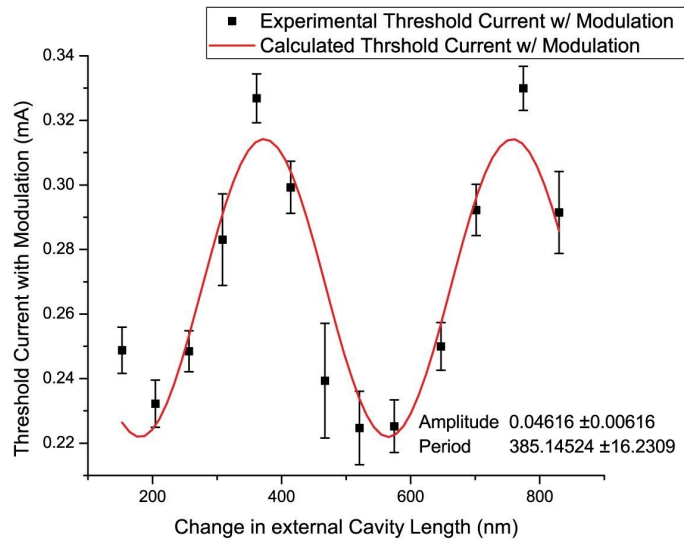


Figure 4.7: Variation of the Threshold Current with Modulation with changing External Cavity Length

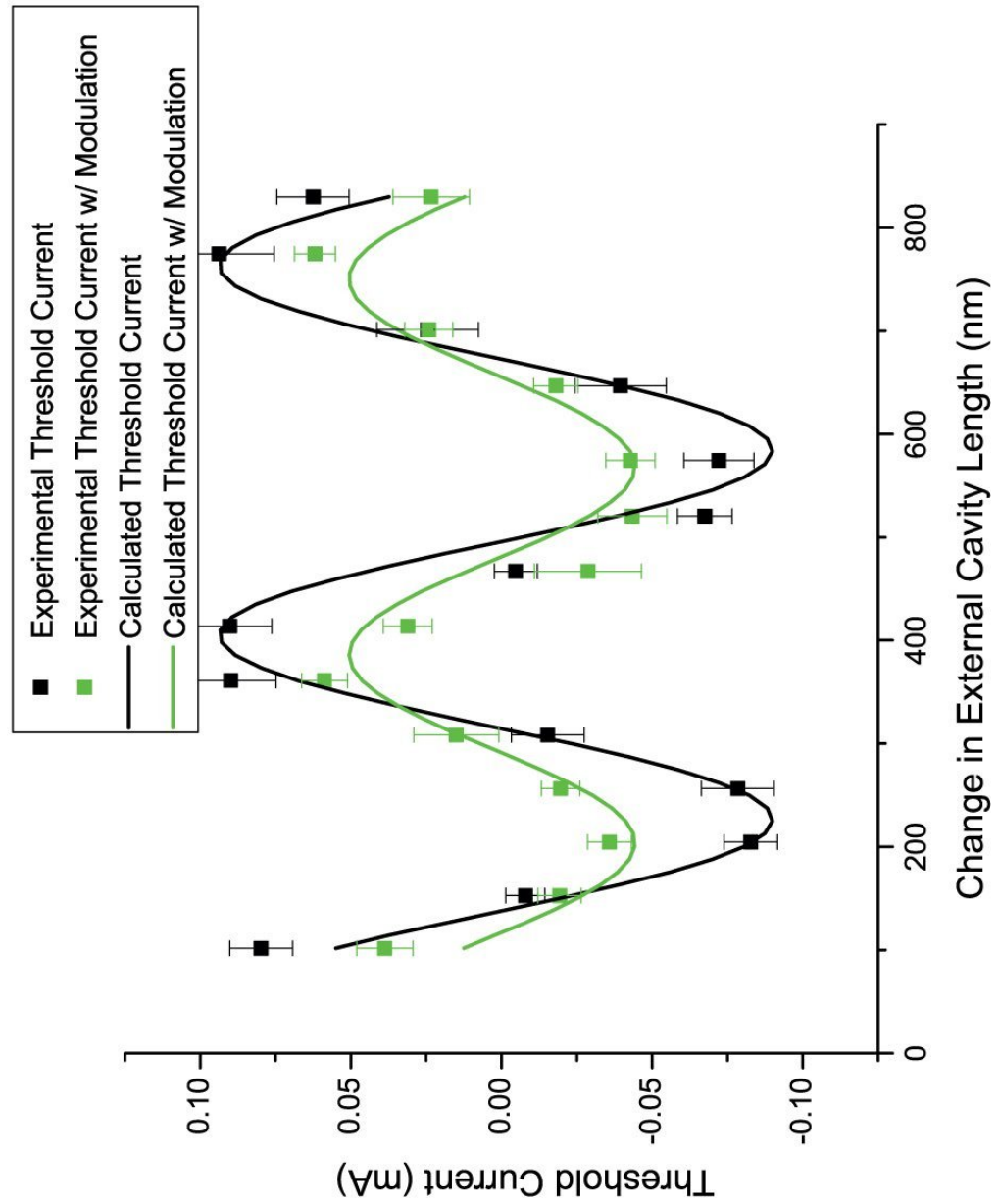


Figure 4.8: Comparison of the Amplitudes of the with and without modulation cases of the Threshold Current variation with Feedback

## 4.5 Threshold Current

Figure 4.6 is a plot of the VCSEL's threshold current with feedback as a function of the change in external cavity length. The plot shows a sinusoidal variation of the threshold current with respect to the change in external cavity length, as was predicted by the rate equations in Ch.3. The upper limit of the period of oscillation within error is approximately 373 nm. The period of oscillation was predicted to be half the wavelength of the laser. Thus, Figure 4.6 predicts the lasing wavelength of the laser to be 746 nm, while the VCSEL lases at 850 nm. The approximately 12% error is most likely due to imprecision in the actuators controlling the position of the fiber. The period of the threshold current oscillation is still in good agreement with the feedback theory from Ch.3.

Figure 4.7 is a plot of the VCSEL's threshold current with feedback and modulation with respect to the change in external cavity length. The threshold current still has a sinusoidal relationship to the external cavity length. In this case the upper limit of the period of oscillation within error is approximately 401 nm, yielding a predicted lasing wavelength of 802 nm. The error with respect to the actual lasing wavelength of 850 nm is approximately 5.6%. The sinusoidal behavior and the oscillation period are in reasonable agreement with the theoretical model from Ch.3 for an unmodulated VCSEL with feedback. Thus, both the cases with and without modulation exhibit sinusoidal behavior

and have approximately the same period. However, a cursory comparison of Figure 4.6 and Figure 4.7 seems to show a difference in the amplitudes of the two plots.

Figure 4.8 is a plot of the threshold current variation for both the with and without modulation cases. The vertical offsets of both have been subtracted to overlay the two plots without changing the amplitude of either. The amplitude of the with modulation case is approximately 60% of the amplitude of the without modulation case. Thus, the addition of current modulation of the VCSEL seems to decrease the effects of the ESEC feedback.

Figure 4.8 also shows a slight phase difference between the with and without modulation cases. Again, this error is most likely due to drift of the actuators that control the fiber position. The position accuracy over the course of one full run-through of the experiment is not good enough to make any precise conclusions about the phase relationship of the plots.

## 4.6 Power

The output power of the VCSEL also varies sinusoidally with the change in external cavity length as predicted in Ch.3 (Figure 4.9). Figure 4.9 and Figure 4.10 show the various output powers for a constant current of 3.7 mA. The upper limit of the period of oscillation within error predicts a lasing wavelength of 732 nm. The error with respect to the actual lasing wavelength of 850 nm

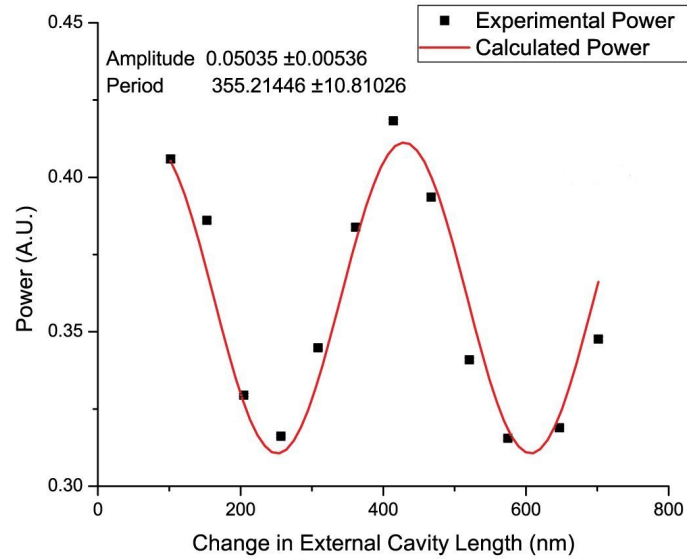


Figure 4.9: Variation of the Output Power with changing External Cavity Length

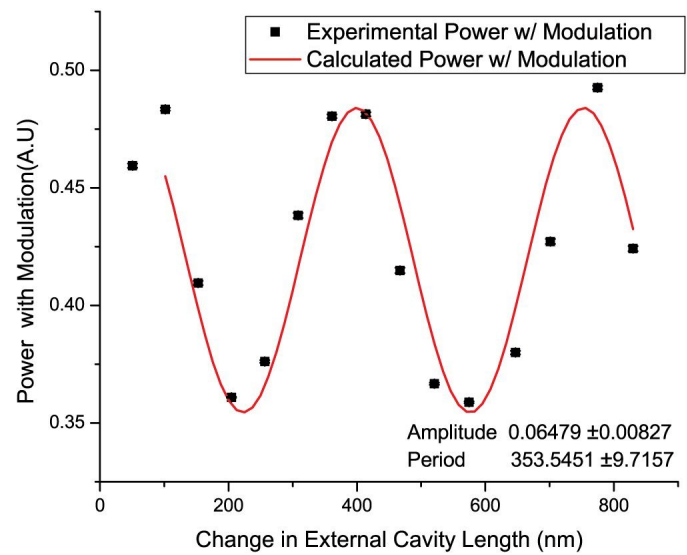


Figure 4.10: Variation of the Output Power with Modulation with changing External Cavity Length

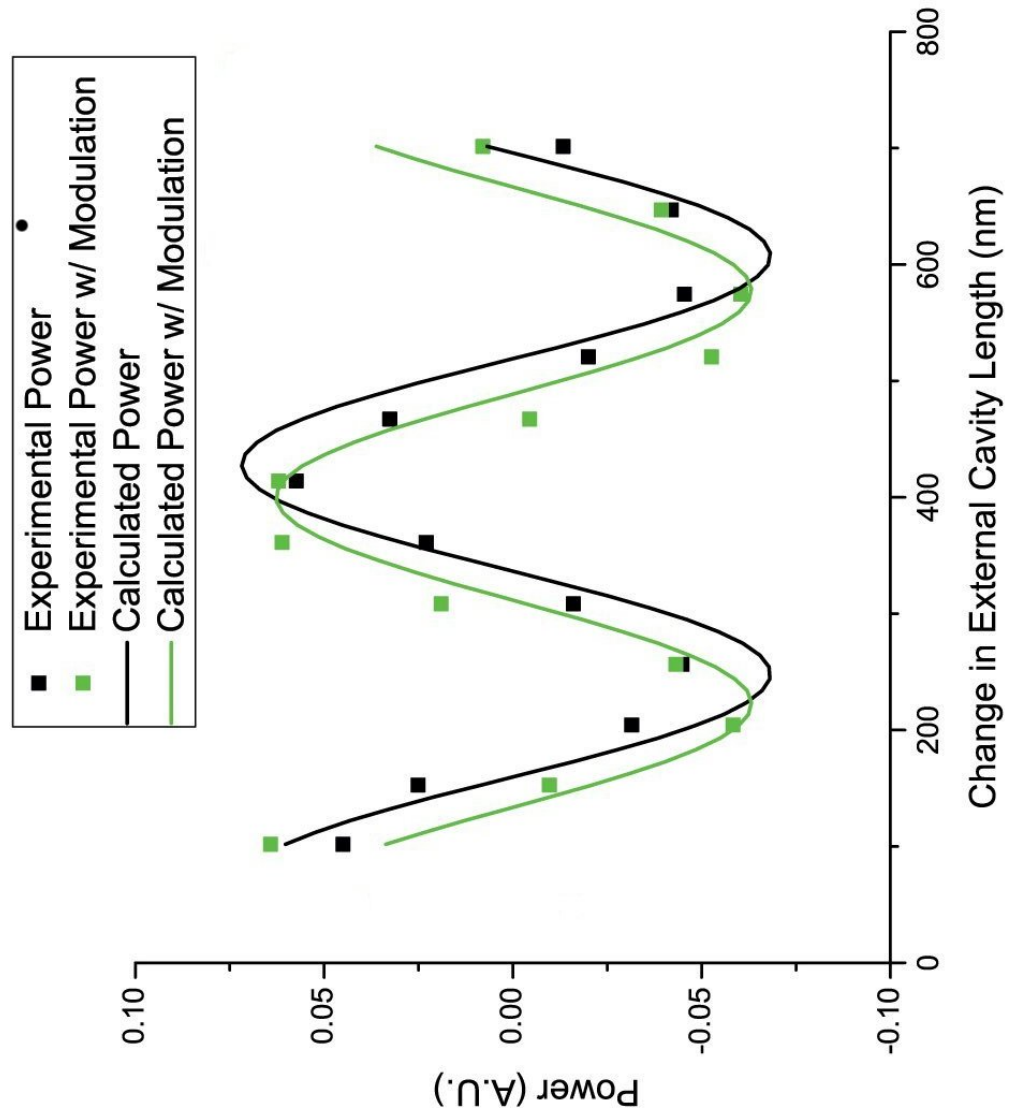


Figure 4.11: Comparison of the Amplitudes of the with and without modulation cases of the Output Power variation with Feedback

is approximately 13.9%. Similarly, the VCSEL with feedback and modulation case, Figure 4.10, still shows a sinusoidal variation of the output power with respect to the external cavity length. The upper limit of the period of oscillation predicts a lasing wavelength of 727 nm, with an error of 14.5%. Thus, ESEC feedback into an unmodulated VCSEL creates no significant deviation from the behavior of the VCSEL with just feedback.

As with the analysis of the threshold current, Figure 4.11 shows a comparison of the amplitudes of the variation for the cases with and without modulation. At 3.7 mA the amplitude of both cases seem to be the same. Unfortunately, the power detector records the root-mean-square of the total output power when the VCSEL is modulated; the recorded output power is effectively the power at the DC injection current plus the RMS of the AC signal. Thus, the power without modulation at 3.7 mA does not correspond to the power with modulation at 3.7 mA. This is a significant distinction since the amplitude of the power variation depends on the magnitude of the injection current, Figure 4.12 and Figure 4.13. Figure 4.12 shows a comparison of the amplitudes of the power variation with feedback and no modulation for injection currents of 2.0 mA, 3.0 mA, and 3.7 mA. As the injection current increases, so does the amplitude of the sine curves. Similarly, Figure 4.13 shows a comparison of the amplitudes of the power variation with feedback and modulation for DC injection currents of 1.0 mA, 2.0 mA, 3.0 mA, and

3.7 mA. Again, the amplitudes of the sine waves increase with increasing DC injection current. Thus, any comparison of the power magnitudes for the with and without modulation cases needs to account for the effective offset of the injection current due to modulation.

Another factor in the magnitude of the output power of the VCSEL is the slope of the LI curve above threshold. The larger the slope of the LI curve the larger the magnitude of the power at any point on the curve. Figure 4.13 shows a comparison of several LI curves with feedback for both the unmodulated and modulated cases. These LI curves correspond to the 5th, 8th, 10th, and 12th points from the left in Figure 4.6 through Figure 4.13. Figure 4.14 demonstrates that the slopes of the LI curves with modulation do not necessarily equal the slopes of the LI curves without modulation. The LI curve for Point 10 demonstrates this most sharply, while the slopes of both cases for Point 8 seem to be equal. This variation in the difference between the slopes of the with and without modulation cases also makes it difficult to justify directly comparing the amplitudes of the powers of the two cases, even if the effective current offset due to modulation is already accounted for.

Even though an absolute comparison of the power variation amplitudes for the with and without feedback cases is problematic, it is still possible to make some general comments about the relative behavior of the VCSEL in both cases. Since the amplitude of the feedback effects increase with increasing

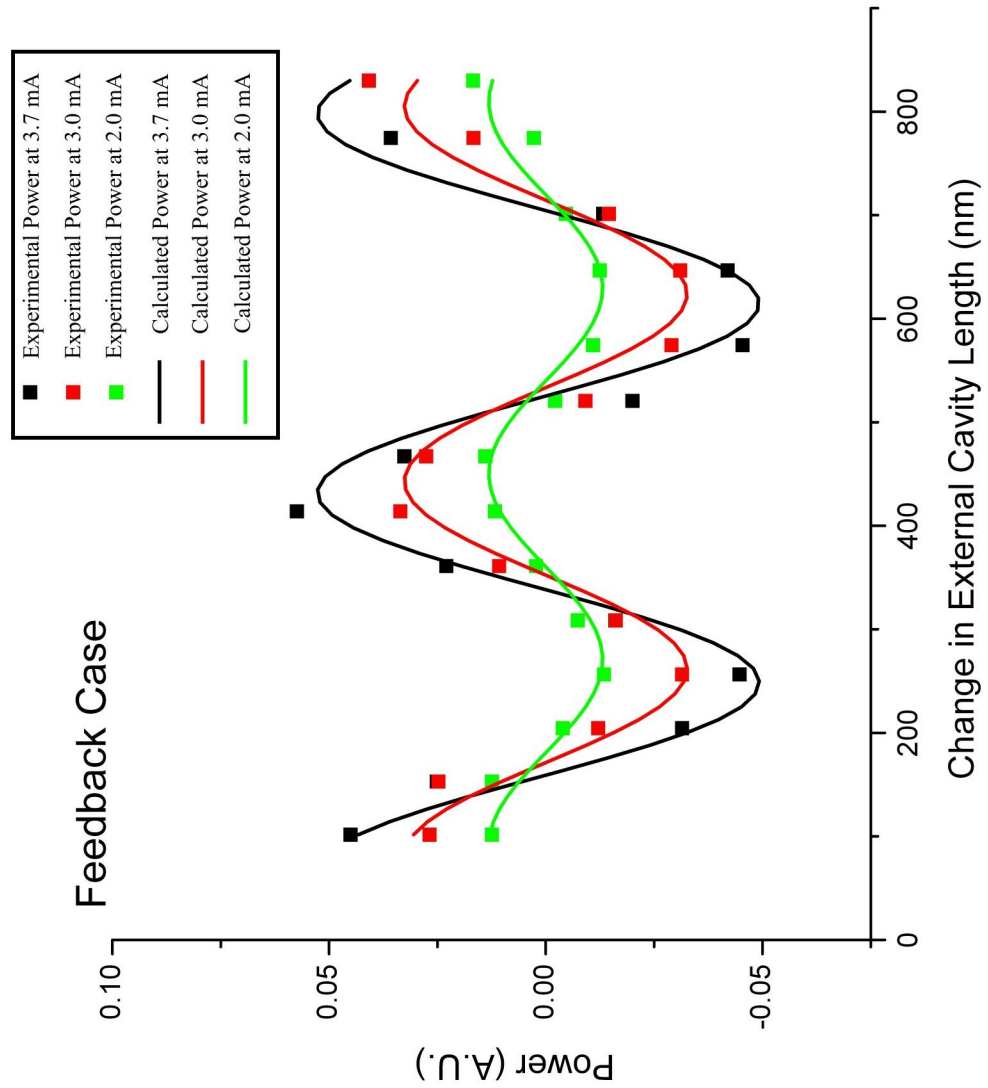


Figure 4.12: Comparison of the amplitudes of the Power variation with feedback for a range of injection currents.

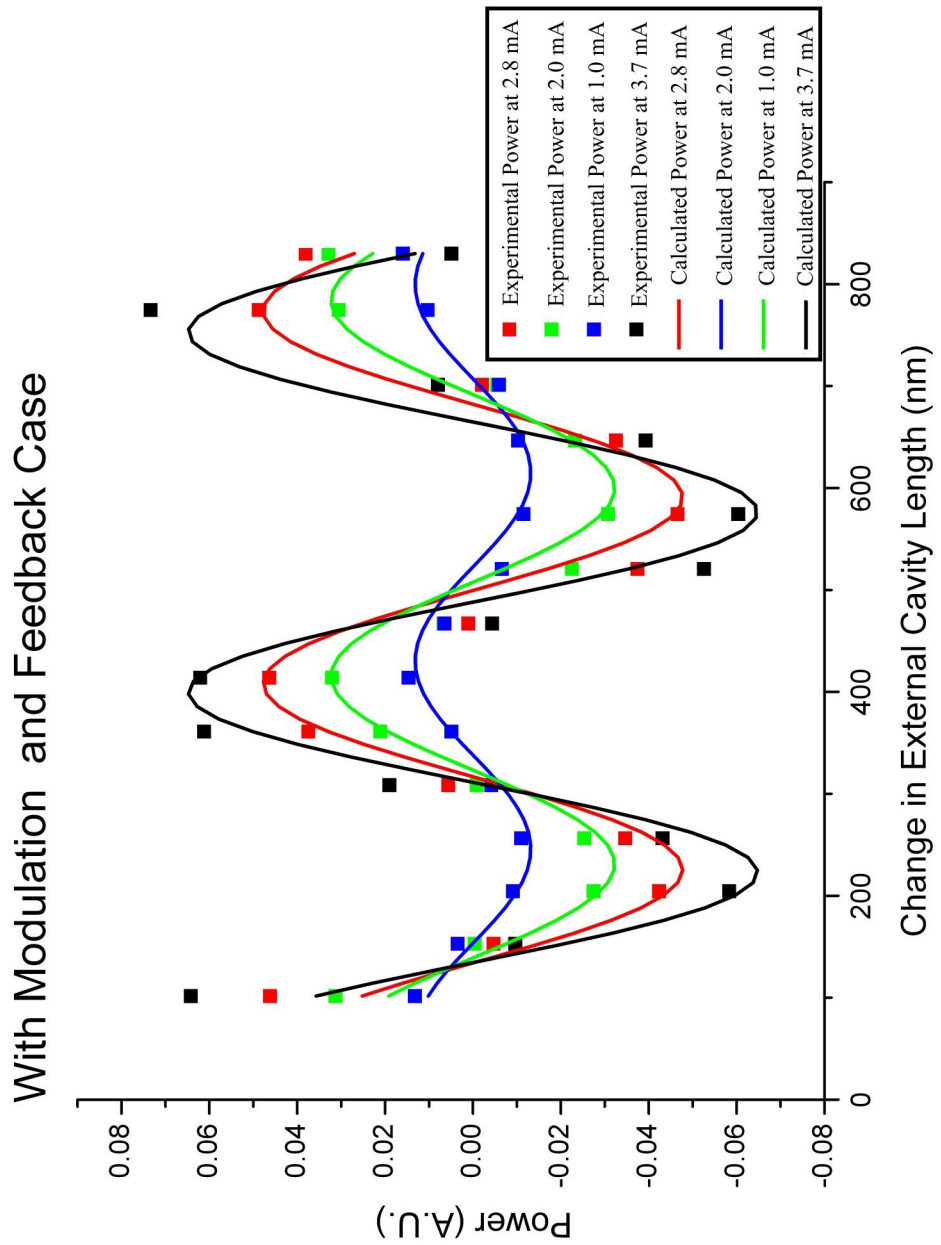


Figure 4.13: Comparison of the amplitudes of the Power variation with feedback and modulation for a range of injection currents.

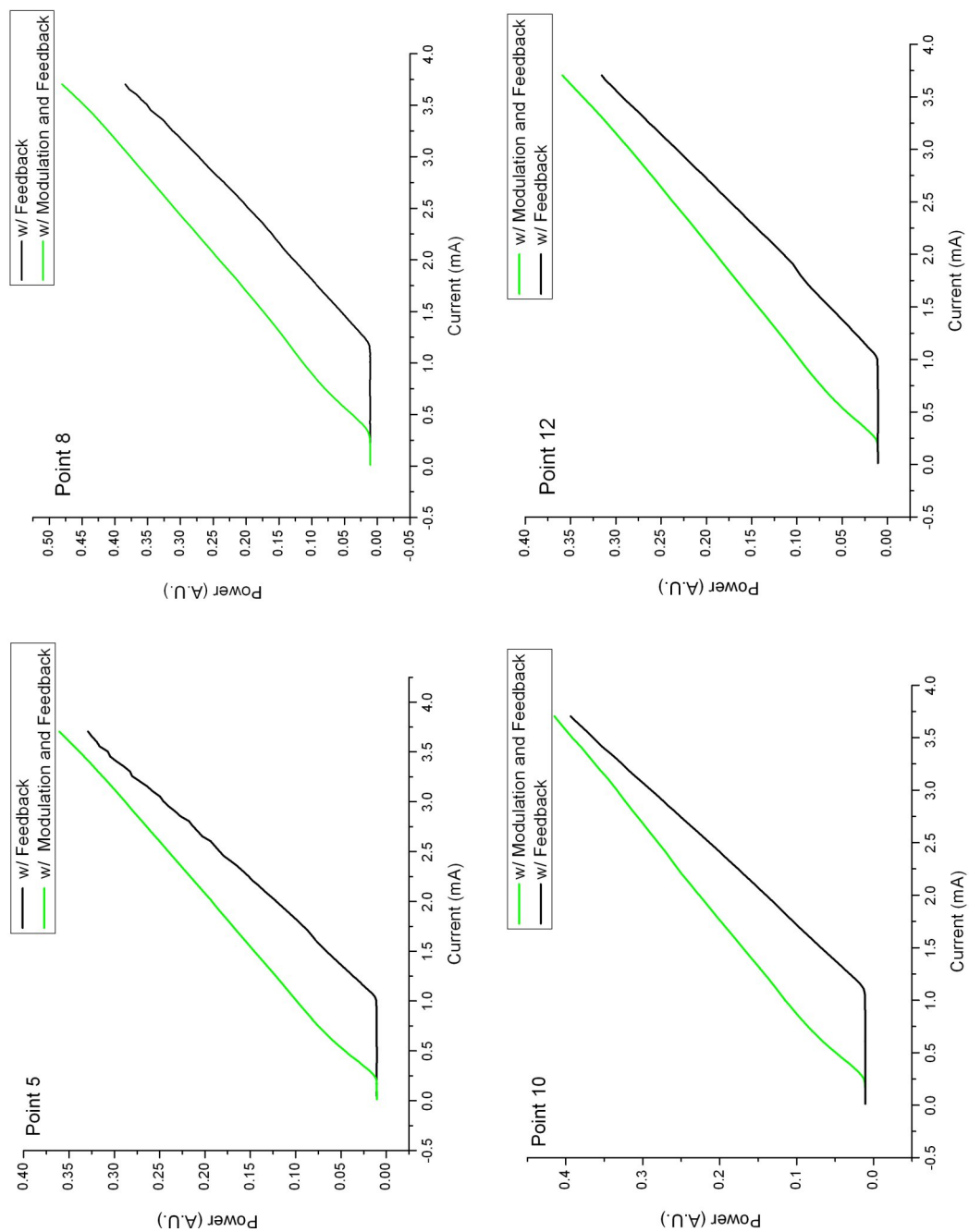


Figure 4.14: Comparison of the slopes of the LI curves with feedback for 4 different trials

injection current, the feedback effects for the case with modulation should always be larger than the effects for the case without modulation. This may not be the case if the magnitude of the power with modulation is smaller than the power without modulation, but Figure 4.13 indicates that even though modulation may cause a decrease in the slope of the LI curve, the power with modulation is still greater than the power without modulation. Thus, if the amplitudes of the power variations are compared for the same injection current, the amplitude of the modulation case serves as an upper limit on the magnitude of the feedback effects on a modulated VCSEL. Therefore, Figure 4.11 does indicate that the effects of feedback on the VCSEL do not increase with the application of a modulated injection current.

## 4.7 Wavelength

Finally, Figure 4.15 shows a variation in lasing wavelength with feedback with respect to change in external cavity length. The lasing wavelength predicted by the period of oscillation is approximately 751 nm, yielding an error of 11.6%. Thus, the experimental wavelength variation is in reasonable agreement with the feedback model. Correspondingly, Figure 4.16 shows a variation in the lasing wavelength with feedback and modulation. The period of oscillation of Figure 4.16 predicts a lasing wavelength of approximately 804 nm with a 5.41% error. Again, modulation of the VCSEL with ESEC feedback caused

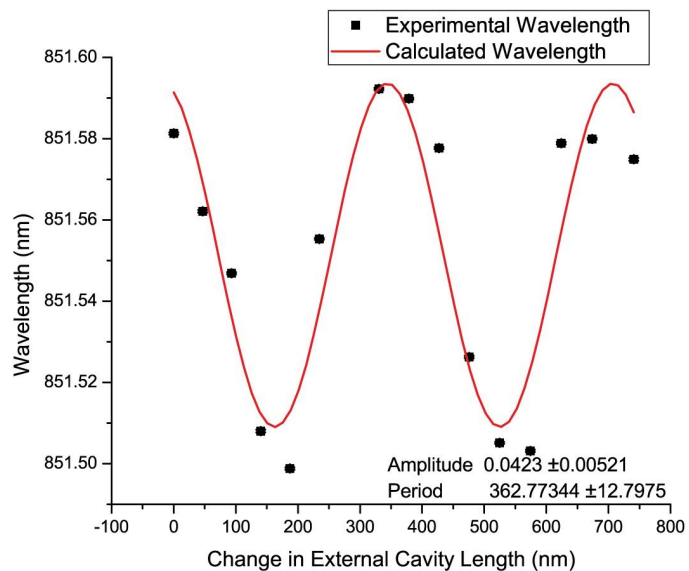


Figure 4.15: Variation of the Lasing Wavelength with changing External Cavity Length

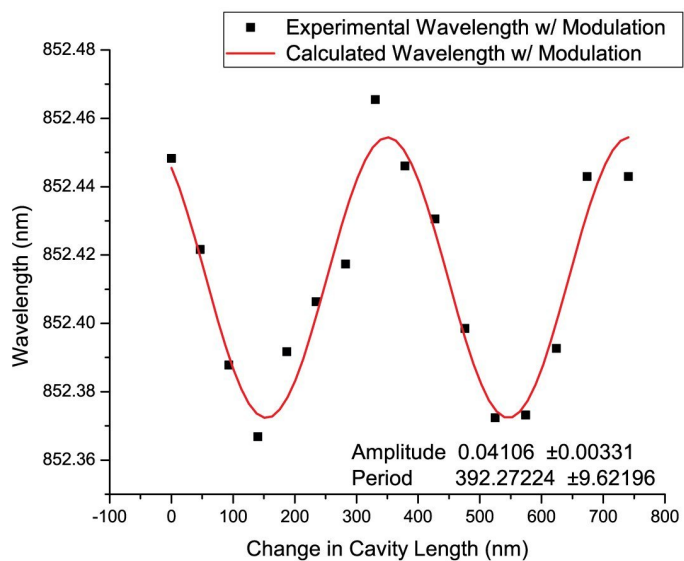


Figure 4.16: Variation of the Output Power with Modulation with changing External Cavity Length

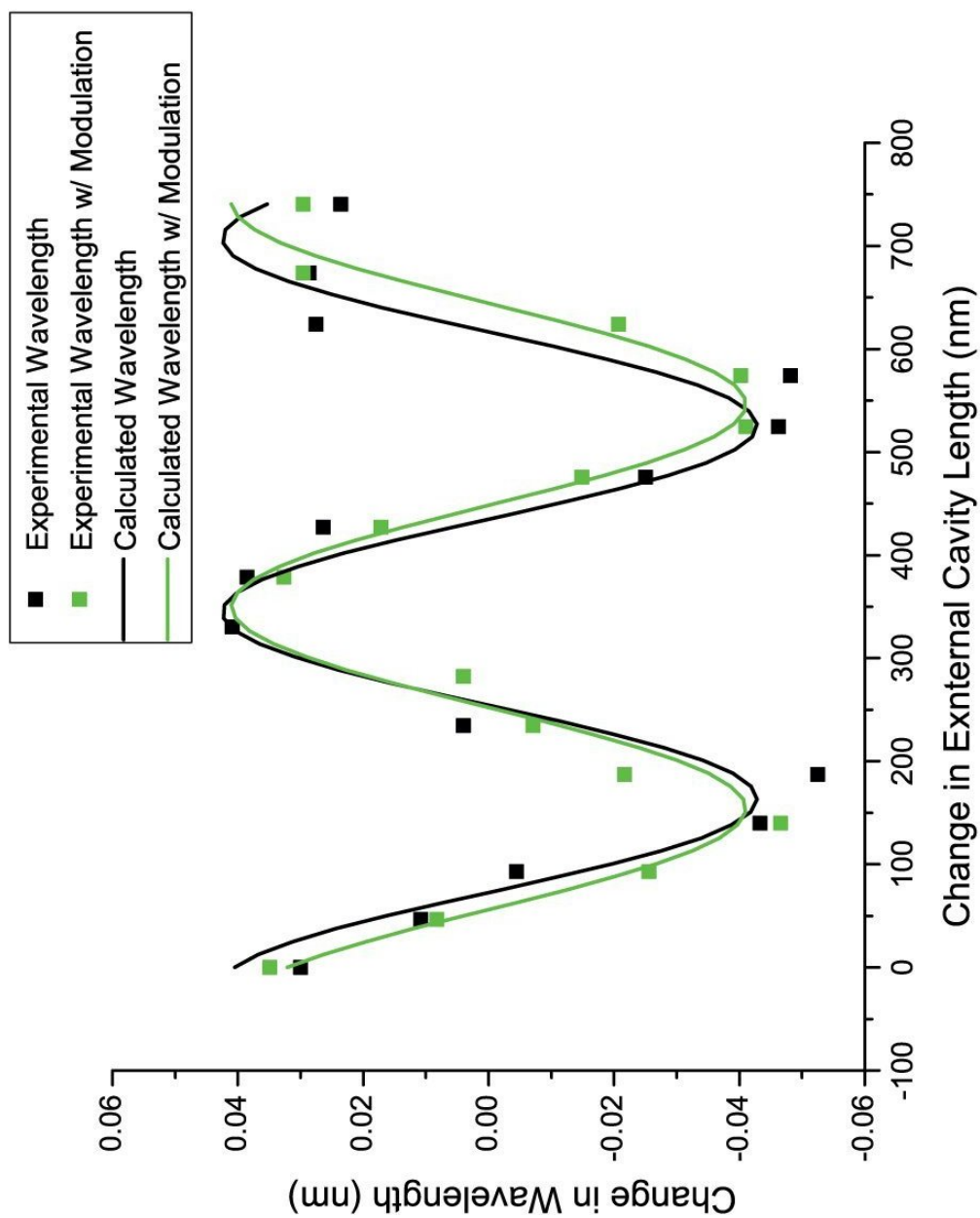


Figure 4.17: Comparison of the Amplitudes of the with and without modulation cases of the Lasing Wavelength variation with Feedback

no significant changes in the behavior of the VCSEL.

[1,3] have also predicted a phase shift between the wavelength variation and the threshold current modulation. As stated previously, the fiber position in the experimental setup undergoes enough drift over the course of the experiment to make any analysis of the phase relationships of the various curves unjustifiable. Thus, any examination of the phase relationship between the threshold current and wavelength shift is beyond the scope of this paper.

Similar to the magnitude of the power, the magnitude of the wavelength depends on the injection current. An increasing injection current causes a redshift of the lasing wavelength. Since both Figure 4.15 and Figure 4.16 show the wavelength variations at a constant DC injection current of 4.008 mA, the two curves do not correspond to the same total injection current. However, as in Section 4.6, the amplitude of the with modulation case at 4.008 mA can be compared to the without modulation case at 4.008 mA if the amplitude of the with modulation case is taken as an upper limit of the effects of modulation on the feedback behavior of the VCSEL. Thus, the comparison of the amplitudes of the two cases shown in Figure 4.17 indicates that modulation does not increase the effects of ESEC feedback into a VCSEL.

## Chapter 5

# CONCLUSION

Modulation was shown to broaden the spectral width of the VCSEL and correspondingly decrease the VCSEL's coherence length. The decrease in coherence length should decrease the effects of the ESEC feedback on the VCSEL by decreasing the strength of the phase relationship between the light in the lasing cavity and the back-reflected light.

To support this hypothesis, modulation of a VCSEL with ESEC feedback was shown to decrease the amplitude of the threshold current variation with respect to changing external cavity length.

Modulation of a VCSEL with ESEC feedback was also shown to not increase the effects of feedback on the VCSEL for a constant DC injection current. While this does not directly indicate a decrease in the effects of feedback on a VCSEL with modulation it does leave open the possibility.

[3] also suggests a decrease in the feedback effects, due to the addition of current modulation, on a semiconductor laser because of a reduction in RIN noise. However, the broadening of the spectral width strongly suggests that the decrease in feedback effects is due partly, if not completely, to the decrease of the VCSEL's coherence length.

Modulation was also shown to destroy the polarization selectivity of the VCSEL with and without feedback, thus making any effects of ESEC feedback on the polarization switching current and polarization switching current hysteresis width of the VCSEL moot.

Therefore, VCSELs are still a viable, low-cost alternative to EELs for use in telecommunications.

# Bibliography

- [1] A. Hsu, J. F. P. Seurin, S. L. Chuang, and K. D. Choquette, "Optical Feedback in Vertical-Cavity Surface-Emitting Lasers," *IEEE Quantum Electron.* **37**, No. 12 (2001)
- [2] M. A. Arteaga, H. J. Unold, J. M. Ostermann, R. Michalzik, H. Thienpont, and K. Panajotov, "Investigation of Polarization Properties of VCSELs Subject to Optical Feedback From an Extremely Short External Cavity - Part II: Experiments," *IEEE Quantum Electron.* **42**, No. 2 (2006)
- [3] K. Petermann, "External Optical Feedback Phenomena in Semiconductor Lasers," *IEEE J. Sel. Top. Quantum Electron.* **1**, No. 2 (1995)
- [4] L.A. Coldren, and S. W. Corzine, *Diode Lasers and Photonic Integrated Circuits*, New York: Wiley, 1995
- [5] S. Jiang, Z. Pan, M. Dagenais, R. A. Morgan, and K. Kaojima, "Influence of External Optical Feedback on Threshold and Spectral Characteristics

- of Vertical-Cavity Surface-Emitting Lasers," *IEEE Photon. Technol. Lett.* **6**, No.1 (1994)
- [6] S. Jiang, M. Dagenais, and R. A. Morgan, "Spectral Characteristics of Vertical-Cavity Surface-Emitting Lasers with Strong External Optical Feedback," *IEEE Photon. Technol. Lett.* **7**, No. 7 (1995)
- [7] Y. C. Chung, and Y. H. Lee, "Spectral Characteristics of Vertical-Cavity Surface-Emitting Lasers with External Optical Feedback," *IEEE Photon. Technol. Lett.* **3**, No. 7 (1991)
- [8] M. Sciamanna, K. Panajotov, H. Thienpont, I. Veretennicoff, P. Megret, and M. Blondel, "Optical feedback induces polarization mode hopping in vertical-cavity surface-emitting lasers," *Opt. Lett.* **28**, No. 17 (2003)
- [9] M. Y. A. Raja, Y. Coa, G. H. Cooper, A. S. Al-Dwayyan, and C. X. Wang, "Polarization and spectral properties of ion-implanted and oxide-confined vertical-cavity surface-emitting lasers," *Opt. Eng.* **41**(3), 704-710 (2002)
- [10] Y. Hong, S. bandyopadhyay, K. A. Shore, "Spectral signatures of the dynamics of current-modulated vertical-cavity surface-emitting lasers subject to optical feedback," *J. Opt. Soc. Am. B* **22**, No.11 (2005)
- [11] Y. Takiguchi, Y. Liu, and J. Ohtsubo, "Low-frequency fluctuation induced by injection-current modulation in semiconductor lasers with optical feedback," *Opt. Lett.* **28**, No. 17 (1998)

- [12] E. Hecht, *Optics*, 4th ed., Glenview, IL: Addison Wesley, 2002
- [13] A. B. Kaplan, "Investigating the Polarization Properties of Vertical-Cavity Surface-Emitting Lasers," B.A. Honors thesis, Amherst College, 2007
- [14] M. A. Arteaga, H. J. Unold, J. M. Ostermann, R. Michalzik, H. Thienpont, and K. Panajotov, "Investigation of Polarization Properties of VCSELs Subject to Optical Feedback From an Extremely Short External Cavity - Part I: Theoretical Analysis," *IEEE Quantum. Electron.* **42**, No. 2 (2006)
- [15] C. H. L. Quay, "The Effect of Optical Feedback on the Coherence Length of Vertical-Cavity Surface-Emitting Lasers," B.A. Honors thesis, Mount Holyoke College, 2001